DENITRIFYING BIOREACTORS – EXTENDING APPLICATIONS TO STORMWATER

A Dissertation

Presented to the Faculty of the Graduate School

of Cornell University

In Partial Fulfillment of the Requirements for the Degree of

Doctor of Philosophy

by

William T Pluer

May 2018

DENITRIFYING BIOREACTORS – EXTENDING APPLICATIONS TO STORMWATER

William T Pluer, Ph. D.

Cornell University 2018

Denitrifying bioreactors have proven effective at reducing nitrate loads from agricultural tile drainage. However, flows associated with storm events can cause conditions that may decrease the effectiveness of the bioreactors for nitrate reduction by decreasing hydraulic retention time. Stormflow may also shift flow paths, alter chemistry, and cause sloughing of biofilm and microbes in the bioreactor. As storms can contribute significantly to annual loads of excess nitrate, the ability for management practices to address stormflow is crucial.

In this research, field and lab bioreactors were observed during stormflows to compare how performance, as measured by removal rate and removal efficiency, was impacted by varied inflow hydrographs. The field study showed that removal rate significantly increased during peak flows but removal efficiency decreased both during and after storms events. The lab study confirmed this trend and found removal rate was most closely associated with internal flow patterns. When bioreactors exhibited predominantly distributed flow rather than preferential flow, event-averaged removal rate and efficiency were both significantly higher.

Both studies of novel applications of bioreactors in stormwater infrastructure

demonstrated effectiveness beyond agricultural fields with removal rates higher than agricultural bioreactors. The submerged bioreactors reduced nitrate in wet detention ponds below recommended levels within one month of installation. This also reduced chlorophyll-a levels. The ditch bioreactor was able to significantly reduce nitrate loads even during stormflows despite the small size. During peak flows, instantaneous removal rate was orders of magnitude higher than previously reported. This work confirms that denitrifying bioreactors are an effective management strategy for reducing nitrate load in stormwater though peak flow rates can cause disruption of high denitrification. Wider application of bioreactors will reduce excess nitrate pollution reaching receiving water bodies and improve water quality

BIOGRAPHICAL SKETCH

Will's interest in water resources reaches back to fun he had splashing in the creek behind the house as a kid. At every step of the way, he has been supported by his wife, parents, and brother. In addition to his research, Will also spent his time in Ithaca playing and coaching volleyball, hiking with his wife and dog, piddling in the garden, and having fun will all his friends.

This is dedicated to everyone who provided help, support, and encouragement during my research. Also to those working as environmental stewards and anyone who has done overnight sampling.

ACKNOWLEDGMENTS

I would like to thank Todd Walter and Larry Geohring for their guidance and support throughout my PhD. I also thank Ruth Richardson and Rebecca Schneider for their input and advice on this work as well as Scott Steinschneider, Roxanne Marino, Bahar Hassanpour, and Chelsea Morris for their collaborations. Thanks to Erin Menzies Pluer, Lauren McPhillips, Sheila Saia, Natalie Morse, James Knighton, and other members of the Soil & Water Lab that provided assistance in sampling, analysis, and editing. Finally, this work was made possible by funding from USDA NIFA, NRCS-CIG, and NSF IGERT and assistance from Fletcher, Simon, Shree, Ian, Stacey, and Nate.

TABLE OF CONTENTS

LIST OF FIGURES

LIST OF TABLES

LIST OF ABBREVIATIONS

BMP	Best management practice
Chl-a	Chlorophyll-a
DOC	Dissolved organic carbon
HRT	Hydraulic retention time
N	Nitrogen
NH_4^+	Ammonium
NO_3^-	Nitrate
RE	Removal efficiency
RR	Removal rate
SCM	Stormwater control measure
SO_4^{2-}	Sulfate

LIST OF SYMBOLS

α	Alpha, significance level
C_i	Inflow or initial concentration
C_o	Outflow or final concentration
d_i	Water depth at inflow
d_o	Water depth at outflow
ε	Porosity
l	Length
q	Flow rate
V_s	Saturated volume
w	Width

CHAPTER 1

INTRODUCTION TO DENITRIFYING BIOREACTOR TREATMENT OF STORMWATER

Application of excess nitrogen fertilizer and manure has been a long-term practice across a range of landuses. Increased deposition, agricultural intensification, the Haber-Bosch process, and expanding suburban areas have increased biologically available nitrogen in landscapes (Galloway et al., 2003). This has also increased nonpoint nutrient pollution to aquatic ecosystem that receive runoff from human-impacted watersheds. In aquatic systems, excess labile nitrogen, most commonly in the form of nitrate (NO_3^-), can remove previous limitations on algal growth. This can lead to a boom in primary production and eventually eutrophication, which can in turn lead to hypoxia. Prominent examples of this in the USA are the Gulf of Mexico and the Chesapeake Bay (Carpenter et al., 1998; Kemp et al., 2005). While decreased nitrogen use could significantly reduce associated environmental issues, engineered best management practices have been developed to remove excess NO_3^- from runoff before it reaches receiving water bodies.

One of the most cost effective and efficient practices to remove excess NO_3^- is the denitrifying bioreactor. Denitrifying bioreactors are designed to pass high-NO_3^- water through a subsurface chamber of organic carbon, typically woodchips (Schipper et al., 2010). This provides high carbon and the anaerobic conditions ideal for naturally occurring denitrifying microbes. The microbes reduce NO_3^- to dinitrogen gas via the four-step process of denitrification. Bioreactors are mainly used to treat effluent from agricultural tile drains, though they have also been used to effectively

treat wastewater and aquaculture effluent (Oakley et al., 2010; von Ahnen et al., 2016). In a meta-analysis, Addy et al. (2016) found an average removal rate (RR) typically ranging from 3 to 7 g N m^{-3} d^{-1} in bioreactors adjacent to agricultural fields. The high removal of NO_3^- suggests potential for bioreactor application to a wider range of settings and water systems, especially stormwater.

Stormwater is a major contributor of annual NO_3^- loads in agricultural, suburban, and urban landscapes (Miller et al., 2017). Existing stormwater infrastructure also provides convenient opportunities for bioreactor application as retrofits. This includes wet detention ponds, bioretention cells, and roadside ditches. However, stormwater provides several challenges to bioreactors that could limit their use and effectiveness. While stormwater is high in NO_3^- loads, it also has high flow rates, which reduce hydraulic retention time (HRT). This decreases the time that water spends in the bioreactor for treatment and studies have shown this reduces RR (Addy et al., 2016). Stormwater can also disrupt flow paths, flush out dissolved organic carbon and microbial communities, increase dissolved oxygen, and decrease temperature, all of which could have negative impacts on RR.

My PhD investigates hydrology and denitrification in agricultural bioreactors during storm events using higher-frequency field sampling and simulated events in lab-scale bioreactors. Based on observations and models from traditional bioreactors, I then investigate two novel applications of modified bioreactors to treat stormwater in new settings. In order to quantify impacts of stormflow on bioreactors, I monitored in-situ agricultural bioreactors during baseflow and stormflow conditions. I also used lab-scale bioreactors to quantify the effects of storm size, duration and resulting internal

flow patterns. I used these findings to design bioreactors that could treat excess NO_3^- in wet detention ponds and roadside ditches. This work showed that stormwater and stormflow rates lead to higher RR, though removal efficiency decreased. The novel applications also proved effective in limited trials and suggest that the principles of bioreactors could be more widely employed to reduce excess NO_3^- in runoff.

REFERENCES

Addy, K., Gold, A.J., Christianson, L.E., David, M.B., Schipper, L.A., Ratigan, N.A., 2016. Denitrifying bioreactors for nitrate removal: A meta-analysis. J. Environ. Qual. 45, 873–881.

Carpenter, S.R., Caraco, N.F., Correll, D.L., Howarth, R.W., Sharpley, A.N., Smith, V.H., 1998. Nonpoint pollution of surface waters with phosphorus and nitrogen. Ecol. Appl. 8, 559–568.

Galloway, J.N., Aber, J.D., Erisman, J.W., Seitzinger, S.P., Howarth, R.W., Cowling, E.B., Cosby, B.J., 2003. The Nitrogen Cascade. Bioscience 53, 341.

Kemp, W.M., Boynton, W.R., Adolf, J.E., Boesch, D.F., Boicourt, W.C., Brush, G.S., Cornwell, J.C., Fisher, T.R., Glibert, P.M., Hagy, J.D., Harding, L.W., Houde, E.D., Kimmel, D.G., Miller, W.D., Newell, R.I.E., Roman, M.R., Smith, E.M., Stevenson, J.C., 2005. Eutrophication of Chesapeake Bay: historical trends and ecological interactions. Mar. Ecol. Prog. Ser. 303, 1–29.

Miller, M.P., Tesoriero, A.J., Hood, K., Terziotti, S., Wolock, D.M., 2017. Estimating Discharge and Nonpoint Source Nitrate Loading to Streams From Three End-Member Pathways Using High-Frequency Water Quality Data. Water Resour. Res. 201–216.

Oakley, S.M., Gold, A.J., Oczkowski, A.J., 2010. Nitrogen control through decentralized wastewater treatment: Process performance and alternative management strategies. Ecol. Eng. 36, 1520–1531.

Schipper, L.A., Robertson, W.D., Gold, A.J., Jaynes, D.B., Cameron, S.C., 2010. Denitrifying bioreactors—An approach for reducing nitrate loads to receiving

waters. Ecol. Eng. 36, 1532–1543.

von Ahnen, M., Pedersen, P.B., Hoffmann, C.C., Dalsgaard, J., 2016. Optimizing nitrate removal in woodchip beds treating aquaculture effluents. Aquaculture 458, 47–54.

CHAPTER 2

STORMFLOW IN AGRICULTURAL DENITRIFYING BIOREACTORS

Introduction

Denitrifying bioreactors have been proven effective at reducing labile nitrogen (N) loads from agricultural tile drainage effluent. These systems provide conditions that are optimal for denitrification: organic carbon and high nitrate (NO_3^-) in an anaerobic environment (Schipper et al., 2010). Within the bioreactors, a community of naturally occurring microbes breaks down complex carbon in woodchips and uses NO_3^- as the electron acceptor. Due to the conditions inside bioreactors, they denitrify at rates significantly higher than natural analogs such as wetlands and riparian areas (Seitzinger et al., 2006). In their review, Addy et al. (2016) reported the average removal rate (RR) from field studies around the world to be 4.7 g N m^{-3} d^{-1} compared with around 0.5 g N m^{-2} d^{-1} in wetlands and riparian areas.

Hydraulic retention time (HRT) is an important factor determining RR based on research at both lab and field scales (Greenan et al., 2009; Christianson et al., 2011; Ghane et al., 2015; Hoover et al., 2016). Hoover et al. (2016) showed removal efficiency (RE) increased with HRT but RR remained constant. Similarly, Lepine et al. (2016) found RE increased though they found RR was optimal with HRT between 5 and 10 hr. Studies like these use a common grab sampling method where inflow and outflow samples are collected simultaneously at regular intervals, often weekly or monthly, throughout the growing season to calculate RR and RE. These are likely accurate assessments of RR during stable environmental and flow conditions in the bioreactors; however, they may not effectively address periods with variable

conditions. Compared with steady-state, variable hydrology is likely to create disturbance in the bioreactor that could reduce denitrification (Song et al., 2010). Christianson et al. (2011) simulated variable flows in pilot-scale bioreactors and found these performed worse than bioreactors with constant HRTs. Bioreactors with upstream containment and steady release had an average RR more than three times larger than those that experienced without inline flow attenuation before inflow.

Precipitation events lead to increases in flow rate in the tile drainage system. Field bioreactors with tile drainage influent will likely be affected by these increased flow rates in several ways. Increased flow rate will lead to a slight increase in saturated volume in the bioreactor but will also result in a lower HRT. The storm-induced flow may also bring in warmer or colder water, which would increase or decrease rates of denitrification, respectively (Hoover et al., 2016). Storm water will also affect NO_3^- leaching in the field and concentration and load of inflow NO_3^- to the bioreactor. Studies have shown that some storm events lead to NO_3^- dilution (e.g. Poor and McDonnell, 2007; Miller et al., 2017) while others show increased NO_3^- mass loading (e.g. Correll et al., 1999; Petry et al., 2002; Miller et al., 2017), though there is no consensus on what causes this disparity in behavior.

Nitrate loading during storms likely contributes significantly to annual loads (Christianson et al., 2013a), but few studies have considered how variable hydrology and NO_3^- loading conditions may affect RR in field bioreactors. Moorman et al. (2015) collected composite samples from bioreactor influent and effluent during storm flows in addition to regular baseflow monitoring. They found that the highest 10% of baseflow rates account for 28% of annual N load. While their flow-weighted sampling

design accurately captured RR averaged for the event, the results of the storm-induced flows were not included in their reactor sizing design analysis.

Additionally, composite sampling does not allow any temporal analysis of RR, which is necessary to understand processes during stormflow events. This temporal analysis is necessary for removing the effects of temperature and HRT to focus on the impacts of variability. Time series analysis can also show how rates of change in flow impact RR and how this moves through the bioreactor. Christianson et al. (2013b) found a capacity for flow attenuation that could be particularly relevant for treatment during flow events.

This study explores NO_3^- loading and RR during baseflow and stormflow through field bioreactors. We hypothesized that bioreactors would not perform as well during and directly following high flow events compared with stable baseflow conditions. Using high-frequency monitoring, we also investigated lag time between samples collected at the inflow and outflow to better understand how flow passes through the bioreactor. We speculated that RR calculated with adjustments for lag time would result in lower peak RR but similar event-averaged RR as previously observed average annual RR. We expected that annual averages of RR considering RR decreases in stormflow periods would be significantly lower than previous estimates based on grab samples alone.

Methods

This study used four bioreactors previously studied (Hassanpour et al., 2017) to provide a comparison between the common sampling technique and higher

resolution sampling of storm runoff. Watershed and bioreactor construction details for the pair of bioreactors in both Chemung and Tompkins counties of New York State are in Hassanpour et al. (2017). At each site, one bioreactor contained woodchip media while the other contained woodchips and biochar mixture at a 9:1 volumetric ratio. Due to minor differences observed in previous study (Hassanpour et al., 2017), these were treated as replicates (R1 and R2, respectively) for this study. The bioreactors were not modified for this study though instrumentation and sample analyses were adjusted to meet requirements of the increased sampling plan. Sites were monitored April to November of 2015. HOBO rain loggers were installed at each site to verify that sampling was triggered by storm-induced events. Telog™ and Onset pressure were placed in each drainage box to continuously measure water temperature and depth over weirs.

ISCO 3700 autosamplers fitted with water level actuators were installed at each drainage control box in April 2015. The actuators triggered ISCO sampling when water levels increased. These were adjusted weekly to be 0.5 cm above the current water level to account for seasonal fluctuations in the water table. Samplers were programmed to collect 200 mL samples at initiation and every 30 minutes after, compositing 4 samples per bottle until all 24 bottles were full. This provided a two-hour resolution of NO_3^- dynamics for 48 hours during and after stormflows. Bottles were pre-acidified to preserve NO_3^- concentration and samples were filtered and refrigerated at 4°C within 72 hours of collection. Bi-weekly grab samples were also collected throughout the monitoring period as baseflow samples that also allow comparison of techniques. These samples were processed similarly to the storm

samples for consistency. Samples were analyzed colorimetrically for combined nitrate-nitrite nitrogen (NO_3^--N) (O'Dell, 1993) and ammonium (NH_4^+) (Bower and Holm-Hansen, 1980).

Storm events where the inflow sampler was not initiated or samplers did not collect at least five samples were excluded from analysis. Flow rate and HRT were calculated using weir calibrations as described by Hassanpour et al. (2017). The average between observed inflow and outflow water depths was used to determine the effective saturated depth in the bioreactors for these calculations allowing for variable volume (Equation 1 and 2). This was then used to calculate RR (Equation 3). Additionally, RE was calculated to account for storms of various sizes and NO_3^- loading (Equation 4). Event averages of both RR and RE were calculated and both time series and event averages were used in analysis. In the equations below, V_{sat} is the saturated volume in the bioreactor, d_i and d_o are the water depth at the inflow and outflow control structures, respectively, l and w are the length and width of the bioreactor, ε is the bioreactor porosity, q is the flow rate, and C_i and C_o are the NO_3^- concentrations at the inflow and outflow, respectively. A value of 0.6 was used for the media porosity as measured by Hassanpour et al. (2017).

$$V_{sat} = \frac{d_i + d_o}{2} * l * w \qquad \text{Equation 1}$$

$$HRT = \frac{\varepsilon V_{sat}}{q} \qquad \text{Equation 2}$$

$$RR = (C_i - C_o) * \frac{q}{V_{sat}} \qquad \text{Equation 3}$$

$$RE = \frac{C_i - C_o}{C_i} \qquad \text{Equation 4}$$

The R software environment version 3.2.1 was used for data and statistical analyses. In paired Mann-Whitney tests, inflow and outflow NO_3^- concentrations were compared to determine if reduction was significant in each bioreactor. Wilcoxon rank-sum tests were used to evaluate comparisons of HRT, RR, and RE between baseflow and event-averaged samples. Time series of flow, HRT, NO_3^- concentration, and temperature at the inflow and outflows were plotted for each event to determine visual patterns in the data. Theoretical values of HRT throughout events were used to determine theoretical lag times identifying when inflow was expected to reach the outflow. When possible, time series were identified where inflow and outflow NO_3^- concentrations or temperature shared obvious breakpoints. These break points were used as a tracer to verify theoretical values. Lag-adjusted values of RR and RE were calculated with outflow concentrations compared with inflow samples collected approximately a lag interval earlier, i.e., in order to try to compare the concentrations in the same water parcel flowing in and out of the bioreactor. These calculations were limited to a 2 hour time resolution. Lag-adjusted RR and RE were compared with previously calculated simultaneous inflow/outflow event means using Mann-Whitney tests.

To better understand how storm events affect annual NO_3^- removed, we developed basic models based on observed baseflow and storm event RR and applied this to hourly temperature and flow collected at the sites. Generalized additive models were used to evaluate RR using inputs of NO_3^- inflow concentration, temperature, and HRT. While similar studies have used linear models (e.g. Hoover et al., 2016), the assumptions of multivariate normality and homoscedasticity were violated in this

dataset. Therefore, generalized additive models were used to allow more flexibility in mathematical function. This also did not require transformation of either independent variables or RR. Model 1 was developed based on grab samples only and Model 2 used all data. In Model 3, additional dependent variables were added that quantified the impacts of maximum flow and coefficient of variation during events. These aimed to characterize the hydrologic and physical disruption experienced by bioreactor media during high flow rates. Baseflow samples were assumed to have a coefficient of variation of zero and a maximum flow equal to the observed flow rate. These three models were fit to the observed sample data and then applied to the entire year of monitoring. For annual data to fit the same structure that Model 3 was based on, maximum flow and coefficient of variation were calculated over a rolling 24-hour period. The average NO_3^- inflow concentration observed at each bioreactor during the sampling period was applied to each bioreactor's dataset. Annual RR averages were compared via paired Student t-tests though the sample number (n=4) was small.

Results and Discussion

Removal during Events

We observed 6 and 8 storms in the pair of Chemung bioreactors and 12 events in each of the Tompkins bioreactors for a total of 38 events. Two storms are presented in Figure 2-1. We collected grab samples of baseflow on 13 dates during the 2015 monitoring period at Chemung and Tompkins bioreactors. Each bioreactor showed significant NO_3^- removal for each sampling method ($p<0.01$) (Figure 2-2). The values

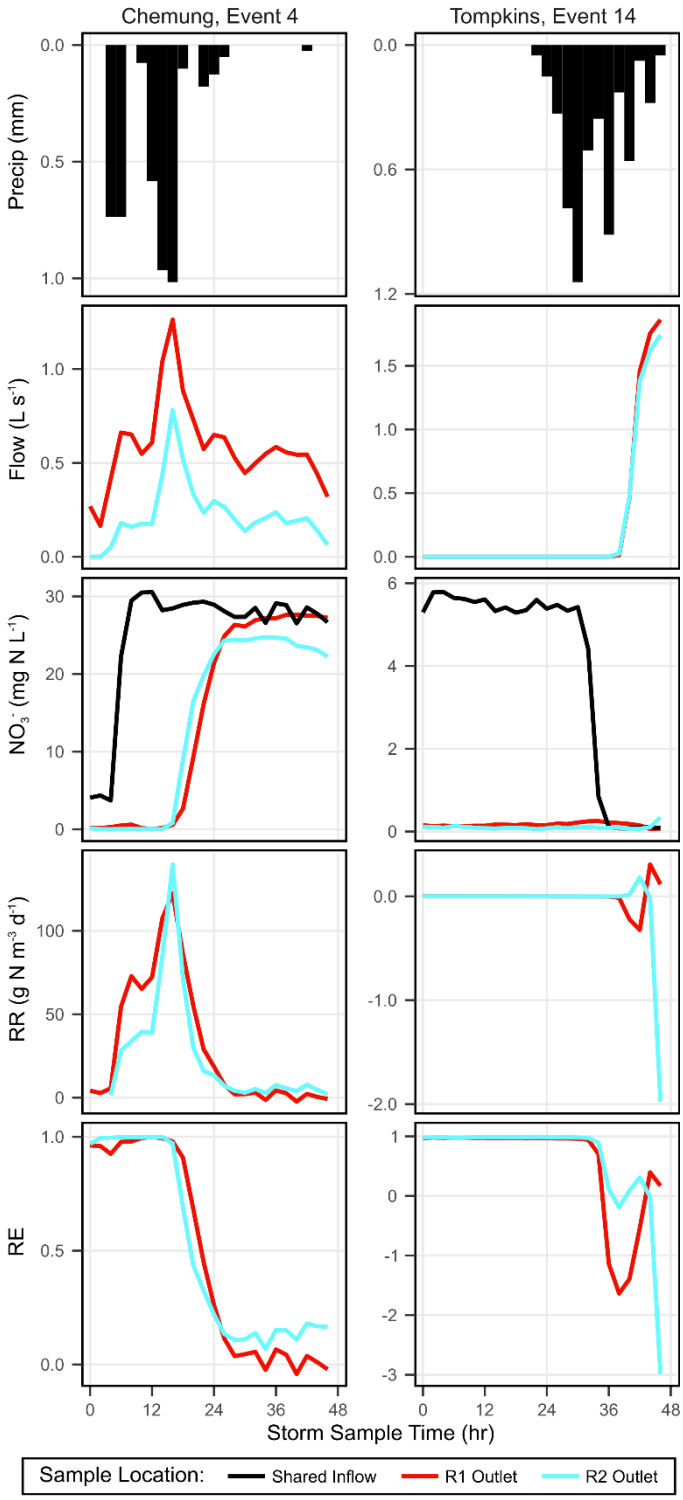

Figure 2-1: Precipitation (a, b), flow (c, d), nitrate (NO_3^-) concentration (e, f), removal rate (RR) (g, h), and removal efficiency (RE) (i, j) for paired bioreactors during two select storms. These selected storms represent only some of the range in storms observed in both sites during the monitoring period. The event at Chemung occurred after a side-dressing and highlights lag observed between inflow and outflow. The Tompkins event occurred after a stagnant period and showed NO_3^- dilution that led to negative values for RR and RE.

for RR and RE calculated from baseflow samples were similar to previous years of monitoring at these sites (Hassanpour et al., 2017).

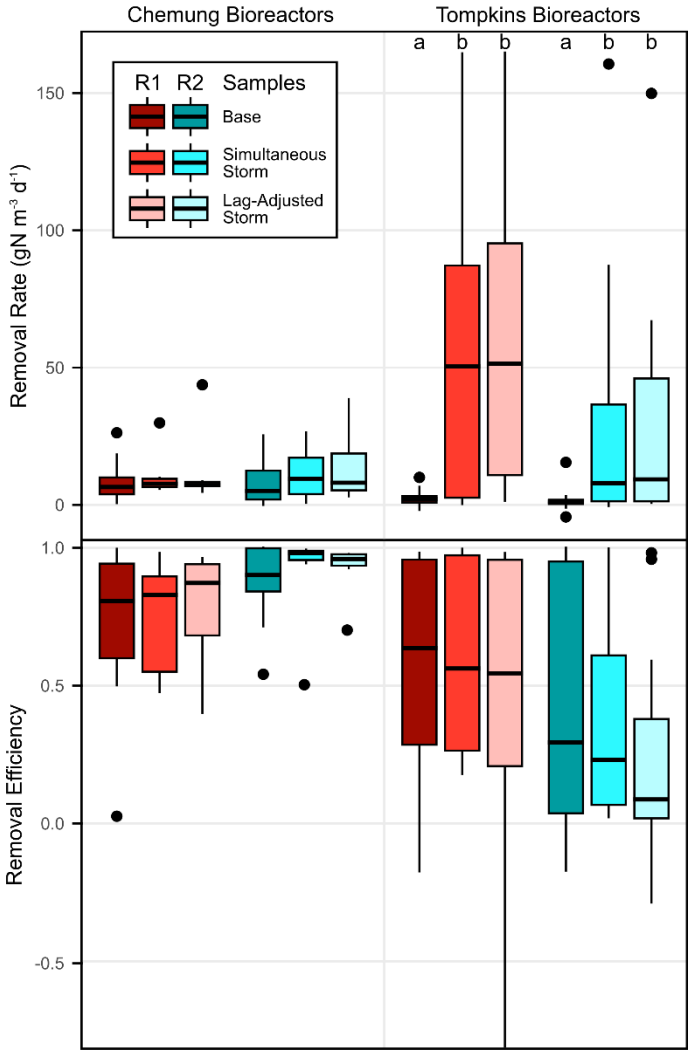

Figure 2-2: Removal rate and removal efficiency of nitrate in paired bioreactors at both sites as sampled during baseflow, storm events analyzed simultaneously, and storm events analyzed with adjustment for lag time. All means were significantly greater than zero. Letters indicate significant difference between means compared within each individual bioreactor ($p<0.05$).

Both Tompkins bioreactors showed significantly higher RR during storm events compared to baseflow sampling. Neither Chemung bioreactor had significantly different RR between storm and baseflow periods, potentially due to the low number of measured storms. Despite increased RR, none of the bioreactors showed

significantly different RE between storm and baseflow monitoring. This may be because of wide variability in RE or because flow is the main driver in increased RR. Flow being the main driver would suggest high RR is caused by hydrology and not increased rates of denitrification. This would also explain why the Chemung bioreactors had lower RRs, as they had some bypass flow during events and did not experience flows as extreme as the Tompkins bioreactors (coefficient of variation in flow of 0.11 and 0.06 in Chemung bioreactors compared to 3.4 in each Tompkins bioreactor).

While RR increased during storms, RR following storm events was significantly less than prior to the storm for two of the bioreactors (Figure 2-3). This suggests that some feature of stormflow causes a disturbance in bioreactor function that persists beyond the high flow rate. This could be due to shifting flow paths, introduction of oxygen, flushing of dissolved organic carbon, or sloughing of biofilms, all of which have been documented in previous research. RR typically recovered prior to sampling the following week suggesting an average recovery time between 2 and 7 days after a storm. With only NO_3^--N concentrations, we were unable to quantify the ratio of complete to incomplete denitrification that occurred during storm events. It is likely that factors that caused a reduction in removal rate also caused a decrease in the ratio of complete denitrification. This would result in higher emission of nitrous oxide, a potent greenhouse gas and intermediate product of denitrification.

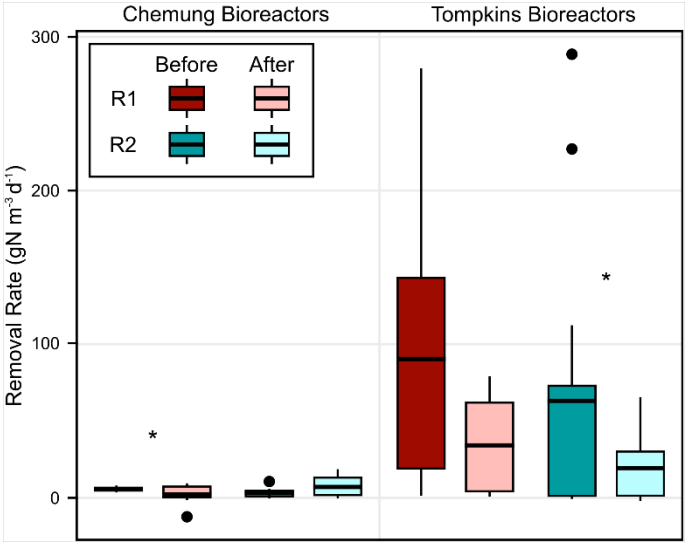

Figure 2-3: Removal rate of nitrate in paired bioreactors at both sites compared at the beginning and end of each storm sampling. Stars indicate significant difference in the mean between sampling before and after the storm event.

Lag Time

Lag times were calculated for 35 of the 38 monitored storms. These ranged from 2 to 24 hours while the remaining three events had lag times greater 40 hours which did not result in a breakthrough during the monitoring period. There were five instances where sharp changes in inflow NO_3^- concentration or temperature were observed in both the inflow and outflow, allowing a tracer-like comparison (e.g. Figure 2-1a). These instances of observed delay values were within one sample period (2 hours) of calculated theoretical lag time. This check supported our calculations, but could not be analyzed quantitatively with only five occurrences among the four monitored bioreactors.

Lag-adjusted event means of RR and RE are compared with event means using simultaneous sampling in Figure 2-2. This omits data from the three storms for which

lag time could not be calculated because it was longer than the monitoring period (e.g. Figure 2-1b). A pairwise Mann-Whitney test of RR averaged by event indicated that lag-adjusted RR was significantly higher than simultaneous RR ($p=0.006$). RE comparisons of event averages were also significant ($p=0.003$). During the few events that showed sharp changes in inflow NO_3^- concentration, event-averaged RR was lower for the lag-time adjusted calculation compared with the simultaneous calculation. This suggests that considering lag time may be important only in situations where inflow NO_3^- concentration is variable and sampling interval is shorter than the lag time, similar to the event observed in Figure 2-1a.

Models and Scaling

Using only grab sample data, a generalized additive model (Model 1, Table 2-1) explained 67% of the variation of RR, with inflow NO_3^- concentration and site being the significant and largest contributors. The significance of inflow NO_3^- concentration may indicate that bioreactors are NO_3^--limited during baseflow; this was observed in previous studies as summarized by Addy et al. (2016). HRT was not significant, which is potentially the result of a small range of observed values during baseflow samples. Model 2, which included event-averaged storm data, was less effective, explaining only 31% of variation in the dependent variable (Table 2-2). In this model HRT, temperature, and site were all significant ($p<0.005$). Temperature had a positive coefficient, as expected (Hoover et al., 2016), but the coefficient for HRT was negative, indicating inverse correlation. This is counter to most studies of HRT

and is further evidence that high RR is likely driven by high flow and not a large reduction in concentration from increased denitrification.

Table 2-1: Model 1 formula and significance of each input variable. This model used 48 data points, had an adjusted R^2=0.63, and explained 67% of deviance. * indicates significance at α=0.05.

RRo ~ HRT + Temp + NO3i + Site + Reactor

Parametric coefficients	Estimate	Std. Error	t value	p value
(Intercept)	0.03	3.08	0.01	1E+00
HRT	-0.04	0.03	-1.22	2E-01
Temp	0.02	0.21	0.08	9E-01
NO3i	1.55	0.21	7.24	7E-09*
Site	-11.63	1.67	-6.95	2E-08*
Reactor	-0.08	1.25	-0.06	1E+00

Table 2-2: Model 2 formula and significance of each input variable. This model used 83 data points, had an adjusted R^2=0.26, and explained 31% of deviance. * indicates significance at α=0.05.

RRo ~ HRT + Temp + NO3i + Site + Reactor

Parametric coefficients	Estimate	Std. Error	t value	p value
(Intercept)	-50.05	16.85	-2.97	4E-03*
HRT	-0.45	0.16	-2.77	7E-03*
Temp	4.57	1.03	4.42	3E-05*
NO3i	0.21	0.71	0.30	8E-01
Site	24.28	6.78	3.58	6E-04*
Reactor	-6.49	6.46	-1.01	3E-01

Table 2-3: Model 3 formula and significance of each input variable. This model used 83 data points, had an adjusted R^2=0.55, and explained 58% of deviance. * indicates significance at α=0.05.

RRo ~ HRT + Temp + NO3i + Site + Reactor + Qmax + Qvar

Parametric coefficients	Estimate	Std. Error	t value	p value
(Intercept)	-17.33	14.40	-1.20	2E-01
HRT	-0.32	0.13	-2.49	2E-02*
Temp	1.58	0.96	1.65	1E-01
NO3i	0.08	0.56	0.14	9E-01
Site	1.07	10.28	0.10	9E-01
Reactor	-6.54	5.08	-1.29	2E-01
Qmax	2.26	1.41	1.60	1E-01
Qvar	67.67	9.67	7.00	9E-10*

In Model 3, variables were included in the generalized additive model to quantify potential disruption due to changing flow (Table 2-3). These were flow variance and peak flow during the event. The new model was able to explain 58% of the full data set. Coefficient of variance was highly significant ($p<0.0001$) though the peak flow was not ($p=0.11$). HRT was also significant in this model and was minimally correlated with peak flow (cor=0.17).

The coefficient estimate for flow variance was positive and large, indicating RR increases as variance in flow experienced by the bioreactor increases. This suggests that periods of high variability should be considered differently, a feature that the first two models were unable to do. Variability may force preferential flow paths within bioreactors, cause sloughing of biofilms and flushing of dissolved organic matter, or cause oxygen penetration into the bioreactor. However, this model indicates that higher variability increases RR. This could be due to increased dispersion within the bioreactor or more effective volume usage. It is unclear exactly what this variable may be identifying as a driver in NO_3^- removal but it shows that it is an important measure to consider for models and annual scaling.

All three models were used to calculate annual average RR based on hourly temperature and flow data, with disruption calculations for Model 3 as described above. Storm events accounted for approximately 49% and 59% of the annual inflow at the Chemung and Tompkins sites, respectively. Annual RR values are summarized for all four bioreactors in Figure 2-4 using each of the three models. This shows that considering RR during storm events can increase predictions for annual RR, especially when considering additional flow metrics beyond HRT. Despite very large standard

deviations, all means were significantly greater than zero ($p<0.05$). These models did not account for low RR caused by NO_3^- limitation as described by Addy et al. (2016). Removing storm events for which any or average inflow NO_3^- concentration were below 2 mg N L^{-1} would remove many of the lower RR values which would likely result in stronger model fits.

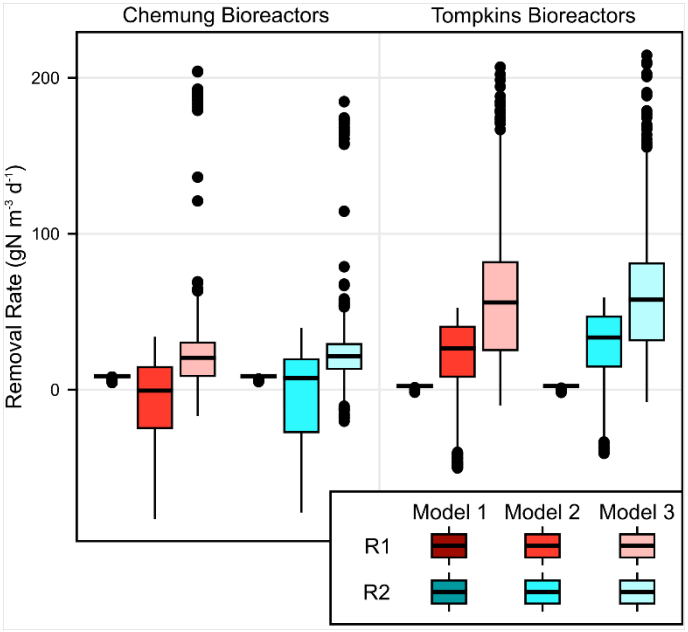

Figure 2-4: Removal rate of nitrate in paired bioreactors at both sites modeled using generalized additive models 1, 2, and 3. Negative values indicate that that the model predicted outflow concentration higher than inflow concentration.

Extensions

The data and models are counter to our hypothesis that RR would decrease during storm flows. This was most likely driven by high RR caused by high flow rates which overcame any decrease due to disturbance or lower rates of denitrification. The high RR during high flow events suggests that the bioreactors are designed larger than they need to be for baseflow conditions and that they are able to treat periodic higher loads.

These findings concur with recommendations for bioreactor sizing developed after installation, which suggest targeting baseflow conditions in order to treat 60% of annual flow volume (NRCS, 2015). Based on these sizing criteria the bioreactors used in this study are roughly five times larger than necessary.

As suggested by Easton et al. (2015), this overly-large design can result in reducing conditions that can produce unwanted byproducts (e.g. methyl-mercury and hydrogen sulfide). In agricultural fields where the major portion of the NO_3^- load is in baseflow, smaller bioreactors with bypass drains for high flows can insure quality treatment without storm disturbance or over-design. This design would forgo treatment of diluted flow during events while better treating baseflow. However, for fields where NO_3^- load is mostly during storm events, designs need to allow for sufficient stormflow HRT without excessively large HRTs during baseflow. Options include upstream volume control to attenuate flow for a smaller bioreactor or draining the bioreactor between events.

Conclusions

Storm flow can account for a major portion of annual NO_3^- loads from agricultural fields. While denitrifying bioreactors are able to remove NO_3^- at high rates during stable conditions, it was unclear how storm flows might influence hydrology that drives RR. Our study found that bioreactors were generally not disrupted during stormflows but instead showed elevated RR during storm events. This was significantly higher for half of the monitored bioreactors. Removal efficiency did not increase with high flows, which suggests that high RR is driven by the flow

component of the RR calculation and not concentration reduction. Correcting for lag time between a flow parcel at the inflow and outflow points did not significantly change annual mean calculations. However, models that incorporated metrics of flow variability and potential for disturbance significantly improved and increased RR predictions.

Based on observations of storm events, stormflow could contribute considerably to NO_3^- treatment in bioreactors at an annual scale. However, the increased sampling and processing required to consider annual stormflow can be expensive. This is particularly relevant in watersheds that have the majority of annual NO_3^- outflow load during event flow instead of baseflow.

This study was limited in its ability to reveal particular flow characteristics that affect denitrification and RR in bioreactors. Additions of conservative tracer at the beginning of storm sampling would provide more comparisons between theoretical and observed HRT that could strengthen lag time analysis. Coupled with monitoring wells throughout the bioreactor, conservative tracers could map internal flow patterns and indicate how flow changes throughout events (e.g., Pluer et al., 2018). The next steps in this research would also benefit from the application of nitrogen isotopes to provide analysis of microbial processes and separate them from physical transport through bioreactors. Better understanding of stormflow NO_3^- load and concurrent bioreactor function is necessary for increasingly accurate annual RR estimates in bioreactors and improving bioreactor designs.

REFERENCES

Addy, K., Gold, A.J., Christianson, L.E., David, M.B., Schipper, L.A., Ratigan, N.A., 2016. Denitrifying bioreactors for nitrate removal: A meta-analysis. J. Environ. Qual. 45, 873–881.

Bower, C.E., Holm-Hansen, T., 1980. A Salicylate–Hypochlorite Method for Determining Ammonia in Seawater. Can. J. Fish. Aquat. Sci. 37, 794–798.

Christianson, L.E., Christianson, R., Helmers, M.J., Pederson, C.H., Bhandari, A., 2013a. Modeling and calibration of drainage denitrification bioreactor design criteria. J. Irrig. Drain. Eng. 139, 699–709.

Christianson, L.E., Hanly, J.A., Hedley, M.J., 2011. Optimized denitrification bioreactor treatment through simulated drainage containment. Agric. Water Manag. 99, 85–92.

Christianson, L.E., Helmers, M.J., Bhandari, A., Moorman, T.B., 2013b. Internal hydraulics of an agricultural drainage denitrification bioreactor. Ecol. Eng. 52, 298–307.

Correll, D.L., Jordan, T.E., Weller, D.E., 1999. Transport of nitrogen and phosphorus from Rhode River watersheds during storm events. Water Resour. Res. 35, 2513.

Easton, Z.M., Rogers, M., Davis, M., Wade, J., Eick, M., Bock, E.M., 2015. Mitigation of sulfate reduction and nitrous oxide emission in denitrifying environments with amorphous iron oxide and biochar. Ecol. Eng. 82, 605–613.

Ghane, E., Fausey, N.R., Brown, L.C., 2015. Modeling nitrate removal in a denitrification bed. Water Res. 71, 294–305.

Greenan, C.M., Moorman, T.B., Parkin, T.B., Kaspar, T.C., Jaynes, D.B., 2009.

Denitrification in wood chip bioreactors at different water flows. J. Environ. Qual. 38, 1664–71.

Hassanpour, B., Giri, S., Pluer, W.T., Steenhuis, T.S., Geohring, L.D., 2017. Seasonal performance of denitrifying bioreactors in the Northeastern United States: Field trials. J. Environ. Manage. 202, 242–253.

Hoover, N.L., Bhandari, A., Soupir, M.L., Moorman, T.B., 2016. Woodchip Denitrification Bioreactors: Impact of Temperature and Hydraulic Retention Time on Nitrate Removal. J. Environ. Qual. 45, 803–812.

Lepine, C., Christianson, L.E., Sharrer, K.L., Summerfelt, S.T., 2016. Optimizing Hydraulic Retention Times in Denitrifying Woodchip Bioreactors Treating Recirculating Aquaculture System Wastewater. J. Environ. Qual. 45, 813–821.

Miller, M.P., Tesoriero, A.J., Hood, K., Terziotti, S., Wolock, D.M., 2017. Estimating Discharge and Nonpoint Source Nitrate Loading to Streams From Three End-Member Pathways Using High-Frequency Water Quality Data. Water Resour. Res. 201–216.

Moorman, T.B., Tomer, M.D., Smith, D.R., Jaynes, D.B., 2015. Evaluating the potential role of denitrifying bioreactors in reducing watershed-scale nitrate loads: A case study comparing three Midwestern (USA) watersheds. Ecol. Eng. 75, 441–448.

Natural Resources Conservation Service (NRCS), 2015. Conservation practice standard: denitrifying bioreactor. Code 605.

O'Dell, J.W., 1993. Determination of nitrate-nitrite nitrogen by automated colorimetry. Method 353.2.

Petry, J., Soulsby, C., Malcolm, I.A., Youngson, A.F., 2002. Hydrological controls on nutrient concentrations and fluxes in agricultural catchments. Sci. Total Environ. 294, 95–110.

Pluer, W.T., Steinschneider, S., Walter, M.T., 2018. Understanding complex flow pathways within lab-scale denitrifying bioreactors via conservative tracers. *In review*.

Poor, C.J., McDonnell, J.J., 2007. The effects of land use on stream nitrate dynamics. J. Hydrol. 332, 54–68.

Schipper, L.A., Robertson, W.D., Gold, A.J., Jaynes, D.B., Cameron, S.C., 2010. Denitrifying bioreactors—An approach for reducing nitrate loads to receiving waters. Ecol. Eng. 36, 1532–1543.

Seitzinger, S., Harrison, J.A., Böhlke, J.K., Bouwman, A.F., Lowrance, R., Peterson, B., Tobias, C., Van Drecht, G., 2006. Denitrification across landscapes and waterscapes: a synthesis. Ecol. Appl. 16, 2064–2090.

Song, K., Lee, S.H., Mitsch, W.J., Kang, H., 2010. Different responses of denitrification rates and denitrifying bacterial communities to hydrologic pulsing in created wetlands. Soil Biol. Biochem. 42, 1721–1727.

CHAPTER 3

UNDERSTANDING COMPLEX FLOW PATHWAYS WITHIN LAB-SCALE DENITRIFYING BIOREACTORS VIA CONSERVATIVE TRACERS

Introduction

A denitrifying bioreactor is designed to efficiently treat excess nitrate (NO_3^-) in agricultural tile drain effluent by providing ideal conditions for denitrifying microbes (Schipper et al., 2010). These conditions consist of a saturated and anaerobic carbon source, most commonly woodchips, through which NO_3^--rich water flows. Results from a number of studies show the extent to which this management practice is effective, with removal rates (RR) ranging from 0.3 to 30 g N m^{-3} d^{-1} in bioreactors (Addy et al., 2016).

Lab-scale bioreactors have allowed more controlled investigation of factors that influence RR, with hydraulic retention time (HRT) consistently showing high significance (Hoover et al., 2016; Lepine et al., 2016; Pluer et al., 2016). Most of these studies use upflow column designs with constant head controlling inflow. This reduces the impact of preferential flow paths and stagnant volume that are likely present in horizontal flow through media. Models based on these findings assume bioreactors work as plug flow systems with average HRT approximately equal to theoretical HRT. Further work to understand hydrology in field bioreactors has shown these assumptions do not hold. Christianson et al. (2013) cited non-ideal flow from ineffective volume utilization as a major limitation of NO_3^- removal. Ghane et al. (2016) modeled flow through woodchip bioreactors using the Forchheimer equation. Similarly, Jaynes et al. (2016) used a dual-porosity flow model to effectively describe

patterns of bromide tracer in the outflow. Studies have also suggested that flows change through time due to movement of woodchips or accumulation of sediment, fine particles, or biofilms (Christianson et al., 2016, 2013; Ghane et al., 2016).

The lab experiments also fail to represent environmental and flow conditions experienced by field bioreactors. Field bioreactors have lower RR than lab bioreactors (Pluer et al., 2016) possibly due in part to variable conditions in the inflow that do not allow bioreactors to reach steady state. This variation is significantly driven by storm-induced runoff events that decrease HRT and potentially decrease temperature and increase oxygen (Christianson et al., 2011). In some cases NO_3^- loading during storms accounts for a majority of the annual load (Correll et al., 1999; Moorman et al., 2015; Petry et al., 2002). Other studies have shown that loads may remain constant or drop during storm events due to dilution (Moorman et al., 2015; Poor and McDonnell, 2007).

Attempts to understand the impact of storm hydrology in bioreactors have been limited, with focus split between processes that may occur during storms (Hassanpour et al., 2017; Moorman et al., 2015; Christianson et al., 2013) and designs to avoid resulting issues (NRCS, 2015; Fenton et al., 2016). Hassanpour et al. (2017) observed decreased NO_3^- removal during high flow or flooding events. Christianson et al. (2013) showed ability to decrease the hydrograph peak by flowing through a bioreactor. Neither study quantified impacts of storm flows on RR. Moorman et al. (2015) used automated samplers to collect composited samples of bioreactor effluent during storms to quantify RR during events. While this study showed a significant portion of annual load in large events, it lacked the high-frequency resolution

necessary to understand bioreactor function during events. To date, there has been no quantification of how storm flows affect RR during the storm and how different storm sizes or bioreactor age may influence this.

This study explores flow patterns and NO_3^- removal in bioreactors during storm runoff events. We investigated the coupled storm hydrology and biogeochemistry of lab denitrifying bioreactors with new and aged woodchip media. Flow, tracer, and RR were observed during three simulated storm runoff events and subsequent recovery periods. The goal of this work was to identify characteristics of storm hydrographs that explain conditions in which bioreactors show decreased RR throughout their lifecycle. This could allow real-time estimates of RR in field bioreactors based on their media age and hourly hydrology instead of annual averages. We hypothesized that larger and longer events would be most disruptive for the bioreactors and lead to significantly lower NO_3^- RR. We also hypothesized that this disruption would be less for new woodchips with potentially more available carbon. These hypotheses were not supported by the data, and further data analysis indicated internal flow dynamics of the bioreactors were a primary control of RR.

Methods

We modified six lab bioreactors previously used in Pluer et al. (2016) in May 2016, with changes to media and flow pathways. These experiments evaluate 3-year-old woodchips and new woodchips, each in triplicate, to capture a more holistic view of bioreactor behavior during its lifetime. Perforated tubing was added at the entrance and exit of the bioreactors to disperse inflow and more evenly capture outflow

distributed across the bioreactor width. Tap water augmented with potassium nitrate was pumped through the bioreactors in series to seed similar microbial communities at the experiment outset. Bioreactors were then separated and baseflow conditions of 20 mg N L^{-1} inflow and 12 hr HRT were established. Baseflow conditions were maintained throughout the monitoring period except during simulated storm runoffs.

Two unmonitored simulations of storm runoff events were run during a month period to establish pumping and sampling techniques. One of these storms attempted to hold NO_3^- load constant while flow rate varied. Switching influent source introduced air bubbles into the intake, so this study focuses only on constant concentration inflows. After this start-up, we simulated three events with varied inflow hydrographs based on the unit hydrograph (Dooge, 1959) and the 1-year storm experienced by previously monitored field bioreactors. Design event hydrographs are presented in Figure 3-1.

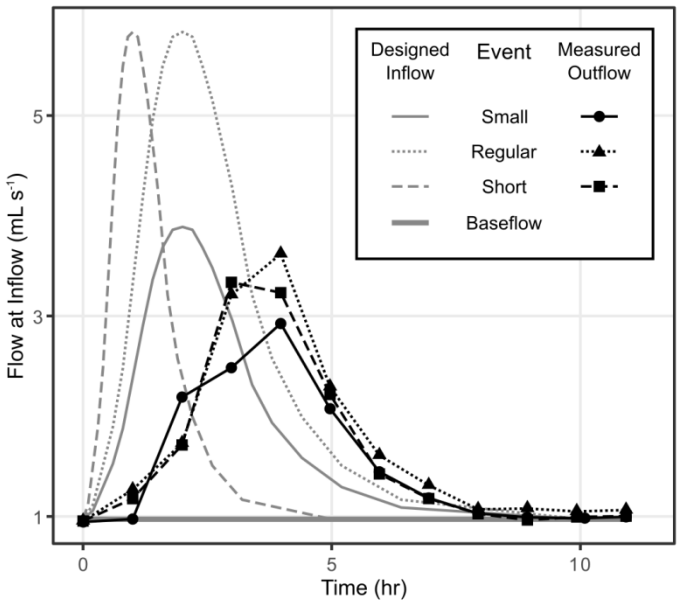

Figure 3-1: Designed inflow and measured outflow rates for three simulated runoff events. Peristaltic pump curves were used to control flow rate and NO_3^- concentration was held constant. Inflow NO_3^- load was proportional to flow rate. Baseflow was maintained between runoff events. Samples were collected for 23 hours after the start of runoff events.

Storm runoff events occurred weekly over the course of 5 to 10 hours. We injected 25 mL of 400 mg L^{-1} bromide solution as an inert tracer at the start of each storm event. This allowed the determination of HRT distribution during the sampling period to ensure each bioreactor performed similarly. Inflow and outflow composite samples were collected hourly for 23 hours after the event began. The samples were filtered using 0.45 µm nylon filters and analyzed for combined NO_3^- and nitrite with colorimetric tests (O'Dell, 1993). Bromide was analyzed via ion chromatography (Pfaff, 1993). Removal rate was calculated as described by Schipper et al. (2010). Removal efficiency (RE) was also calculated to control for varied inflow NO_3^- loading rates. This is the mass of NO_3^- removed per mass of NO_3^- input. With inflow equal to outflow, this can be calculated as the concentration reduction in NO_3^- divided by concentration of NO_3^- in the inflow.

The R software environment version 3.2.1 was used for statistical analysis, which is composed of two primary analyses. First, averages of RR and RE for each individual time series (a particular runoff event in a particular bioreactor, i.e., 18 series in this experiment) were compared by event and media age using two ANOVA models. One was a standard 2-way ANOVA with interaction effects between event and media age, and the other was a mixed-effects ANOVA without an interaction term but with random effects to control for within-subject variability of each bioreactor. Tukey Honest Significant Difference analysis was used as necessary. The ANOVA tests indicated there might be additional controls on RR besides media age and event type. Therefore, we performed K-means clustering on characteristics of the bromide load time series to objectively separate major flow patterns observed, based on

methods used by Chang et al. (2008) and Wang and Zhang (2011). The characteristics used in the clustering analysis were the maximum bromide outflow, time to 50% load, and average HRT, although other metrics (effective volume, Morrill Dispersion Index (Christianson et al., 2013), and short circuiting (Ta and Brignal, 1998)) were also compared across clusters after clusters were determined. Average RR and RE were compared between clusters using a Student t-test. Tests of proportion were conducted to test for significant differences in how time series associated with different events or media ages were grouped into clusters. Results showed that event and media age were not independent from identified clusters, so the interactions between clusters and these factors were evaluated without the use of additional statistical tests (i.e., 3-way ANOVA) to avoid complications of collinearity between factors.

Results and Discussion

Bioreactor Performance during Events

All bioreactors showed NO_3^- reduction during and after all storm runoff events. The average RR during baseflow conditions was 16 g N m^{-3} d^{-1}, which is similar to our previous lab bioreactor study (Pluer et al., 2016). Average RR during simulated event and subsequent sampling periods was 23 ± 2.4 g N m^{-3} d^{-1}. The instantaneous RR increased for all bioreactors during events concurrently with flow (Figure 3-2e). At its peak, RR was more than twice as high as the highest reported annual average by Bell et al. (2015). Removal efficiency decreased during events and increased after a return to baseflow, though it remained high relative to field bioreactors (Addy et al., 2016) (Figure 3-2i). Inflow concentration was constant for all events so decreased RE was

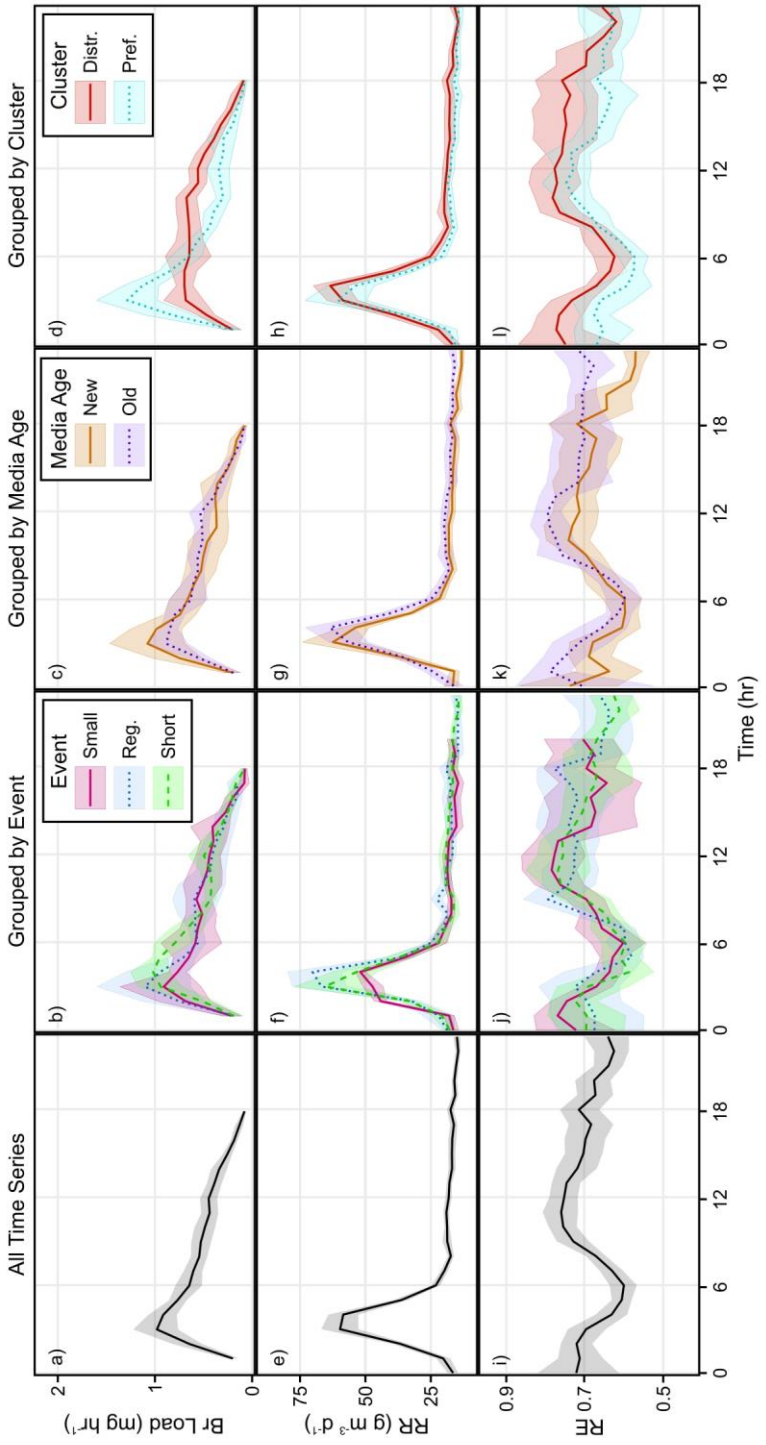

Figure 3-2: Time series grouped by potential explanatory variables. Bromide outflow load (a-d), instantaneous removal rate (RR) (e-h), and removal efficiency (RE) (i-l) were averaged by indicated groupings. Shading shows 95% confidence interval calculated via bootstrapping.

driven by increased NO_3^- concentration in the outflow. This indicates that bioreactors were not able to reduce NO_3^- load as effectively during events compared with baseflow. A greater mass of NO_3^- is removed in the storm, although it is not clear if this is a result of rapidly increased denitrification or microbial uptake and later denitrification (Seitzinger et al., 2006).

Flow rates in all bioreactor outflows were less than estimates, based on peristaltic pump curves. Peak flow in the outflow decreased by an average of 33% and took twice as long to appear (Figure 3-1). Outflow rate returned to baseflow on average two hours later than expected. This confirms that bioreactors can attenuate storm flows with friction through the media and storage as previously shown by Christianson et al. (2013).

Comparison of pre- and post-event performance shows peak flow disrupted bioreactor function. Removal rate and RE is significantly lower immediately following events and at the final sampling than before the event (Figure 3-3a, e). This suggests that all events were sufficiently large to alter bioreactor function for at least 12 hours after the event ended. Previous work (Pluer et al., 2016) showed 1.5 pore volumes were necessary to stabilize NO_3^- concentrations in bioreactor effluent. While the sampling period in this study did not span this period due to the high HRT at baseflow, it did show extended disruption. Performance had returned to base conditions before the start of each subsequent event.

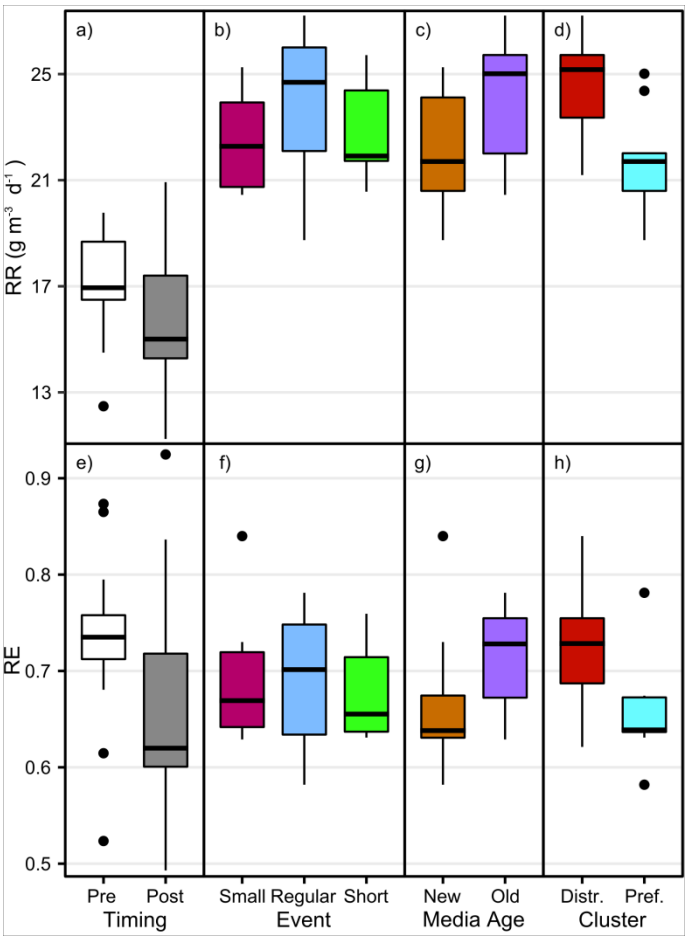

Figure 3-3: Mean removal rate (RR) (a-d) and removal efficiency (RE) (e-h) compared by potential explanatory variables. Bioreactors performed significantly better before events than after. There were no significant differences between events or media age. Clusters were significantly different in both metrics with the distributed cluster performing significantly better than the cluster dominated by preferential flow.

Effects of Media Age and Event Type

The small event showed a lowered bromide peak during peak flow (Figure 3-2b). The decreased peak RR did not result in significantly different event averages (Figure 3-2f, Figure 3-3b). The short event had a shorter duration in peak RR that resulted in a lower average RR (Figure 3-2f, 3-3b). This was also not significantly different from the regular event. Removal efficiency between the three events were

very similar through the time series and showed no significant difference between event averages (Figure 3-2j, 3-3f). The older media showed a lower bromide peak, less variability between replicates, and greater RR during recovery (Figure 3-2c, g). This resulted in a slightly higher but insignificant average RR and RE (Figure 3-3c, g).

The standard ANOVA confirmed that event type was not a significant driver of RR ($p=0.47$). Media age was significant with $p=0.05$. In the Tukey Honest Significant Difference analysis, none of the comparisons of event and media interaction was significant, although it is worthwhile to note that the Tukey test is a less powerful test than ANOVA to identify significant effects. In a mixed-effects ANOVA of RR, events were again insignificant ($p=0.60$), and media age became insignificant ($p=0.14$). Removal efficiency showed no significance of either event type or media age as a driver in either ANOVA model. Overall, the results indicate no significant influence of event type on RR or RE, but suggest a possible effect from media age.

K-means Clustering of Complex Flow Pathways within Bioreactors

Average HRT of the bromide tracer during runoff events was consistently lower than the theoretical value. Percent recovery of the tracer was 86 ± 4%. These are similar to findings from studies using steady flow conditions and may be due to adsorption to woodchips (e.g. Ghane et al., 2015; Jaynes et al., 2016). There were two general patterns of bromide load in the outflow as identified by k-means clustering. These groups explained 65% of the variance for factors quantifying the flow pattern (see Table 3-1). One cluster appears to represent time series dominated by distributed flow while the other cluster consists of time series dominated by preferential flow

early in the storm event (Figures 3-2d). Adding a third group in the clustering analysis increased the variance explained to 79%. In this case, the preferential flow group became more extreme and the third group represented a combination of preferential and distributed flows. This suggests that the flow patterns vary over a gradient rather than across a sharp threshold between distributed and preferential flow paths. However, given the small addition in variance explained when using three groups, two groups were used for the remainder of the analysis.

Table 3-1: Comparison of flow patterns between clusters quantified by various metrics. Values given are cluster mean and standard deviation with p values of significance test of the difference in means.

Metric	Distributed	Preferential	p-value
Hydraulic retention time (hr)	8.3 ± 0.7	6.7 ± 1.0	<0.01[b]
Time to 50% bromide load (hr)	8.6 ± 1.0	5.7 ± 0.9	<0.01[b]
Maximum bromide load (mg hr^{-1})	1.0 ± 0.2	1.4 ± 0.4	0.02[b]
Effective volume	1.7 ± 0.3	1.5 ± 0.3	0.06[b]
Morrill Dispersion Index (Christianson et al., 2013)	4.4 ± 0.8	4.7 ± 0.8	0.38[a]
Short circuiting metric (Ta and Brignal, 1998)	0.5 ± 0.1	0.6 ± 0.1	0.20[b]

[a] indicates p-value from Student t-test
[b] indicates p-value from Wilcoxon rank sum test

Values for various metrics that could describe the different flow patterns are given in Table 3-1. Differences were only significant for average HRT, time to 50% load, and maximum bromide load, the same variables used for the K-means clustering. K-means clustering was also run on all metrics of flow pattern shown in Table 3-1. This did not result in any shifting of time series between groups and less variance (57%) was explained by the groups. Morrill Dispersion Index and the short circuiting metric are both based on empirically derived quantiles, and their interaction with the

peaked time series results in a wide range of values. While more appropriate quantiles could be developed for the lab bioreactors, a larger dataset would be necessary.

Using clustering from K-means clusters, the distributed cluster had significantly higher RR than the preferential flow cluster (Figure 3-3d, 24.4 and 21.7 g N m^{-3} d^{-1}, p=0.01). Removal efficiency was also significantly higher in the cluster dominated by distributive flow (Figure 3-3h, 0.72 compared with 0.66, p=0.04). These differences were not significant at individual time points during events, though the average distributed time series was consistently higher (Figure 3-2h, l).

The distributed cluster consistently performed better than the preferential flow when compared between events or media age. The regular event showed the greatest variability within clusters while the short event showed high homogeneity within clusters and the greatest difference between clusters. The smaller event had more time series that displayed distributed flow. Bioreactors showed the greatest reduction of hydrograph peak flow during this event, which may have resulted in more mixing. In contrast, the short event attenuated flow the least and showed the highest proportion of preferential flow. The proportions were not significant (p=0.51) and differences in flow attenuation were minor. Therefore, it is unlikely that these alone would be enough to drive the degree of difference seen in flow patterns.

The old media tended to display distributed flow patterns more often than the new media, although the difference in proportional test was not significant (p=0.35). The average initial particle size, packing process, and final mass were the same between the two media ages. Research by Ghane et al. (2016) showed that while controlling as many factors as possible, older woodchips have less intrinsic

permeability. This may have occurred in our experiment as well and would account for more dispersive flow. We also attempted account for media settling and establish similar microbial communities within the bioreactors. Both of these would likely impact biofilm formation, which has been shown to affect flow rates (Chun et al., 2009). These results may indicate more time is necessary to establish a robust and diverse microbial community that is able to withstand variable conditions.

In addition, individual bioreactors did not display consistent flow patterns throughout the study. Instead, many switched between clusters for different events – displaying a distributed flow pattern for one event and then preferential flow in the next or vice versa. Bioreactors did not move between clusters with any particular patterns. The seemingly random switching makes it even more difficult to link event size or duration to the flow because bioreactors themselves change through time. It is unclear, due to the limited number of events, whether bioreactors would eventually settle into a particular flow pattern.

Extensions of this Research

The significant difference in treatment between the two flow patterns has large implications for bioreactor research. For instance, in central New York State, runoff events affect 12% of days per year on average (National Oceanographic and Atmospheric Association. National Centers for Environmental Information. Global Historical Climatology Network. Meteorological Station Number USC00304174. 2015. Raw unpublished data.). If bioreactors take about a day to recover, then about one in five days are negatively impacted by event flows. This would reduce annual RR

estimates by 183 g N m^{-3} yr^{-1} and RE by about 1.5% assuming that inflow NO_3^- load is consistent every day. If storm flows increase inflow NO_3^- load, then these reductions in performance would be larger.

It will be important to determine a way to quantify dispersion between bioreactors to compare flow patterns. This study uses relative comparison of flow path characteristics between a small sample of bromide tracer series. A classification model would need to be designed to allow further time series to be categorized as dominantly distributed or preferential flow. This classification model would require a larger sample size and would be best if using metrics that were simple to measure. While this would establish standard thresholds to separate flow patterns, each individual event would need to be monitored and retroactively categorized, which does not improve the predictability of storm outflow or annual estimates.

This study assumes that bromide is an inert tracer that effectively represents flow through porous media as described by Jaynes et al. (2016). It is necessary to understand how NO_3^- may behave differently than bromide in the bioreactors, specifically that microbes may actively uptake NO_3^- and some NO_3^- removal may be associated with incomplete denitrification. Applying the clustering technique to NO_3^- isotope tracer series would highlight transport differences. Simultaneous nitrogen gas measurements would also show the proportion of retained NO_3^- that is being completely denitrified. Increases in emissions of nitrous oxide, a greenhouse gas that is an intermediate product of denitrification, would indicate incomplete denitrification. This would also directly address whether increased RR was due to sorption or increased denitrification.

This technique must also be applied to field bioreactors. Baseflow and storm-induced event flow patterns should be quantified in many bioreactors across a range of media and ages and should measure an entire year of events. The inter-event variability in flow pattern and RR might average out over the span of a year or more. Alternatively, bioreactors could settle into patterns over time. No-till soil management leads to the establishment of semi-permanent preferential flow paths (Andreini and Steenhuis, 1990). This is a likely outcome for undisturbed bioreactor media, although it could be offset by the constantly shifting and settling as woodchips decay. While simulated events were representative of field runoff events scaled by HRT, the actual flow paths in the lab bioreactors are much shorter than in the field. The length of the flow path and the number of woodchips and pores encountered would likely increase dispersion of inflow in the field (Matsubayashi et al., 1997).

To address the uncertainty of when bioreactors will display preferential flow and temporarily decrease RR, future bioreactor designs should install features to generally increase dispersion or flow attenuation. Some recent bioreactors have been installed with baffles to increase the shortest flow path between inflow and outflow. However, in increasing the flow path without changing volume, average pore velocity would increase, which could negatively affect the microbial community by causing biofilm sloughing or flushing of dissolved organic carbon. Performance of modified bioreactors should be studied during runoff events to ensure the gain in dispersion is not offset by increased flow velocity.

Conclusions

Bioreactors were able to treat NO_3^- in storm runoff events. While instantaneous RR tripled, RE dropped during increased flow rates. Both recovered after flow returned to baseflow, although both RR and RE remained significantly lower after events than directly before disturbance. Average RR for the 23-hour period including storm runoff events was greater than at baseflow. Neither event size nor duration were significant predictors of RR and RE, while media age was significant or near significant depending on the statistical test used.

K-means clustering of the time series of bromide load in the outflow described 65% of variation with two dominant flow patterns. The cluster dominated by distributed flow had significantly higher average RR and RE than those with predominately preferential flow. There was a weak association between older woodchips and distributed flow, suggesting a mechanism by which older woodchips influenced RR and RE, although this was not conclusive. In addition, individual bioreactors appeared to randomly switch between clusters from event to event, suggesting that event properties and media age are not a driver of preferential or distributed flow. The strength of significance between clusters and the lack of difference between events suggest that internal flow characteristics play a larger role in NO_3^- removal than external drivers.

In order to better understand event response, further simulations are necessary. These should address the low sample size and lack of replicated storms in different orders. It is also important to include a broader range of hydrograph shapes and investigate the role of other characteristics known to vary during storms, such as

diluted inflow NO_3^- concentration, decreased temperature, and increased dissolved oxygen and organic carbon in the inflow. Finally, future work should consider the variety of bioreactor shapes and designs to determine how length to width ratio, distributive inflow, baffles, and orifice drains impact flow patterns and the resulting NO_3^- removal in event flows.

Storm-induced events account for a significant portion of annual NO_3^- loading to surface water bodies. While denitrifying bioreactors are an effective management practice to reduce NO_3^-, the conditions during storm-induced events change and can negatively affect the rate of denitrification. Improved understanding of RR during events will reduce the negative impacts of the disturbed conditions and allow bioreactors to effectively treat NO_3^- in baseflow and stormflow conditions.

REFERENCES

Addy, K., Gold, A.J., Christianson, L.E., David, M.B., Schipper, L.A., Ratigan, N.A., 2016. Denitrifying bioreactors for nitrate removal: A meta-analysis. *J. Environ. Qual*. 45, 873–881.

Andreini, M.S., Steenhuis, T.S., 1990. Preferential paths of flow under conventional and conservation tillage. *Geoderma* 46, 85–102.

Bell, N.L., Cooke, R.A.C., Olsen, T., David, M.B., Hudson, R., 2015. Characterizing the performance of denitrifying bioreactors during simulated subsurface drainage events. *J. Environ. Qual*. 44, 1647–1656.

Chang, F.J., Tsai, M.J., Tsai, W.P., Herricks, E.E., 2008. Assessing the ecological hydrology of natural flow conditions in Taiwan. *J. Hydrol*. 354, 75–89.

Christianson, L.E., Hanly, J.A., Hedley, M.J., 2011. Optimized denitrification bioreactor treatment through simulated drainage containment. *Agric. Water Manag*. 99, 85–92.

Christianson, L.E., Helmers, M.J., Bhandari, A., Moorman, T.B., 2013. Internal hydraulics of an agricultural drainage denitrification bioreactor. *Ecol. Eng*. 52, 298–307.

Christianson, L.E., Lepine, C., Sharrer, K.L., Summerfelt, S.T., 2016. Denitrifying bioreactor clogging potential during wastewater treatment. *Water Res*. 105, 147–156.

Chun, J.A., Cooke, R.A., Eheart, J.W., Kang, M.S., 2009. Estimation of flow and transport parameters for woodchip-based bioreactors: I. laboratory-scale bioreactor. *Bioprocess Eng*. 104, 384–395.

Correll, D.L., Jordan, T.E., Weller, D.E., 1999. Transport of nitrogen and phosphorus from Rhode River watersheds during storm events. *Water Resour. Res*. 35, 2513.

Dooge, J.C.I., 1959. A general theory of the unit hydrograph. *J. Geophys. Res*. 64, 241–256.

Fenton, O., Healy, M.G., Brennan, F.P., Thornton, S.F., Lanigan, G.J., Ibrahim, T.G., 2016. Holistic Evaluation of Field-Scale Denitrifying Bioreactors as a Basis to Improve Environmental Sustainability. *J. Environ. Qual*. 45, 788.

Ghane, E., Fausey, N.R., Brown, L.C., 2015. Modeling nitrate removal in a denitrification bed. *Water Res*. 71, 294–305.

Ghane, E., Feyereisen, G.W., Rosen, C.J., 2016. Non-linear hydraulic properties of woodchips necessary to design denitrification beds. *J. Hydrol*. 542, 463–473.

Hassanpour, B., Giri, S., Pluer, W.T., Steenhuis, T.S., Geohring, L.D., 2017. Seasonal performance of denitrifying bioreactors in the Northeastern United States: Field trials. *J. Environ. Manage*. 202, 242–253.

Hoover, N.L., Bhandari, A., Soupir, M.L., Moorman, T.B., 2016. Woodchip Denitrification Bioreactors: Impact of Temperature and Hydraulic Retention Time on Nitrate Removal. *J. Environ. Qual*. 45, 803–812.

Jaynes, D.B., Moorman, T.B., Parkin, T.B., Kaspar, T.C., 2016. Simulating woodchip bioreactor performance using a dual-porosity model. *J. Environ. Qual*. 45, 830–838.

Lepine, C., Christianson, L.E., Sharrer, K.L., Summerfelt, S.T., 2016. Optimizing Hydraulic Retention Times in Denitrifying Woodchip Bioreactors Treating

Recirculating Aquaculture System Wastewater. *J. Environ. Qual*. 45, 813–821.

Matsubayashi, U., Devkota, L.P., Takagi, F. 1997. Characteristics of the dispersion coefficient in miscible displacement through a glass beads medium. *J. Hydrol*. 192, 51–64.

Moorman, T.B., Tomer, M.D., Smith, D.R., Jaynes, D.B., 2015. Evaluating the potential role of denitrifying bioreactors in reducing watershed-scale nitrate loads: A case study comparing three Midwestern (USA) watersheds. *Ecol. Eng*. 75, 441–448.

Natural Resources Conservation Service (NRCS), 2015. Denitrifying bioreactor. *Code 605*.

O'Dell, J.W., 1993. Determination of nitrate-nitrite nitrogen by automated colorimetry. *Method 353.2*.

Petry, J., Soulsby, C., Malcolm, I.A., Youngson, A.F., 2002. Hydrological controls on nutrient concentrations and fluxes in agricultural catchments. *Sci. Total Environ*. 294, 95–110.

Pfaff, J.D., 1993. Determination of inorganic anions by ion chromatography. *Method 300.0-2.1*.

Pluer, W.T., Geohring, L.D., Steenhuis, T.S., Walter, M.T., 2016. Controls influencing the treatment of excess agricultural nitrate with denitrifying bioreactors. *J. Environ. Qual*. 45, 772–778.

Poor, C.J., McDonnell, J.J., 2007. The effects of land use on stream nitrate dynamics. *J. Hydrol*. 332, 54–68.

Schipper, L.A., Robertson, W.D., Gold, A.J., Jaynes, D.B., Cameron, S.C., 2010.

Denitrifying bioreactors—An approach for reducing nitrate loads to receiving waters. *Ecol. Eng*. 36, 1532–1543.

Seitzinger, S., Harrison, J.A., Bohlke, J.K., Bouwman, A.F., Lowrance, R., Peterson, B., Tobias, C., Van Drecht, G., 2006. Denitrification across landscapes and waterscapes: A synthesis. *Ecol. Appl.* 16, 2064-2090.

Ta, C.T., Brignal, W.J., 1998. Application of computational fluid dynamics technique to storage reservoir studies. *Water Sci. Technol*. 37, 219–226.

Wang, K., Zhang, R., 2011. Heterogeneous soil water flow and macropores described with combined tracers of dye and iodine. *J. Hydrol*. 397, 105–117.

CHAPTER 4

DENITRIFYING BIOREACTORS REDUCE STORMWATER NITROGEN: A FLORIDA, USA CASE-STUDY

Introduction

Suburban areas have been increasing in population and area in the United States and globally in the past half century and are a significant source of nitrogen (N) in surface water (Carpenter et al. 1998; Bettez and Groffman 2012). Nitrogen pollution in suburban watersheds originates largely from nonpoint sources, primarily N deposition and domestic fertilizers (Lovett et al. 2000; Osmond and Hardy 2004). This contributes to high nitrate (NO_3^-) loads that lead to eutrophication in estuarine and coastal waters (Kemp et al. 2005). Many stormwater control measures (SCMs) treat suburban runoff, including bioretention and wet detention ponds, with denitrification as a major mechanism of NO_3^- removal (Bettez and Groffman 2012).

Wet detention ponds focus primarily on reduction of peak flows and treatment of particulate pollutants. They have little impact on dissolved NO_3^- load (Mallin et al. 1998) and can, instead, require algaecide use to control algae blooms (Collins et al. 2010). Conditions for denitrification are rarely achieved in constructed ponds due to the lack of organic matter in soils used for construction (Mallin et al. 1998). Despite their limited ability to manage nutrient pollution, wet detention ponds are one of the most popular SCMs throughout the United States. Improving their function could have a great impact on water quality. Recent studies investigated potential retrofits for ponds to increase nutrient treatment using floating treatment wetlands (Borne et al. 2013), filtration (Winston et al. 2017), and dredging (Schwartz et al. 2017).

Strategies for NO_3^- removal in other settings may provide insight into improving suburban water quality. Denitrifying bioreactors efficiently reduce NO_3^- in agricultural tile drainage (Schipper et al. 2010). In these systems, high NO_3^- drainage water flows through a saturated bed of woodchips that provide conditions necessary to support denitrifying microbes (e.g. Schipper et al. 2010). Removal rate (RR) in bioreactors range from 1 to 30 g N m^{-3} d^{-1}, with outflow concentrations reduced below 2 mg N L^{-1} in many cases (Bell et al. 2015; Addy et al. 2016). Some studies have effluent NO_3^- concentration much lower than 2 mg N L^{-1}, which could be biologically limiting for denitrification (Addy et al. 2016). Submerged denitrifying bioreactors in wet detention ponds could provide similar conditions to field bioreactors and could produce similar rates of denitrification.

This study investigates how modified denitrifying bioreactors for wet detention ponds could reduce NO_3^- and algae in ponds to decrease downstream nutrient pollution and improve pond aesthetics. Two bioreactors were installed in ponds near the Florida Gulf Coast and were monitored for a year. Nitrate concentrations were expected to decrease at RRs comparable to field bioreactors.

Methods

Pond Selection

Eight candidate ponds in suburban areas near Sarasota, Florida were chosen based on characteristics common in Florida, including pond surface area, depth, contributing drainage area, and land use. All ponds were in housing developments surrounded by fertilized lawns. Runoff served as the major source of water and

nutrient influx. Ponds did not receive chemical herbicide applications in the year prior to or during the study. This common practice inhibits algae growth and could confound chlorophyll-a (chl-a) results. Initial grab samples were collected from prospective bioreactor installation locations from the eight ponds in August 2013 and analyzed as described below (data not shown).

Two wet detention ponds were selected (labeled A and B, Figure 4-2) based on levels of NO_3^- and chl-a that were notably higher than natural ponds in the region (Florida DEP, 2015). Bioreactor location in each pond was determined by sampling access and proximity to electricity to power pumps. We also selected locations in narrower portions of the ponds to amplify the effects of the bioreactors during the sampling period. Full transect samples were conducted in October 2013 for selected ponds to establish pre-installation conditions (Table 4-1, top portion).

Bioreactor Construction and Installation

The bioreactors were designed based on those used in agricultural applications. Each bioreactor consisted of an iron framework, lined with geotextile fabric to contain the woodchips (Figure 4-1). A 2-inch perforated pipe, running the entire length of the bioreactor, was set in place when half of the bioreactor was filled with woodchips to ensure the pipe was centered in reactor. This was connected with inflow plumbing to facilitate radial inflow along the length of the bioreactor. More information on construction are provided in Table 4-1.

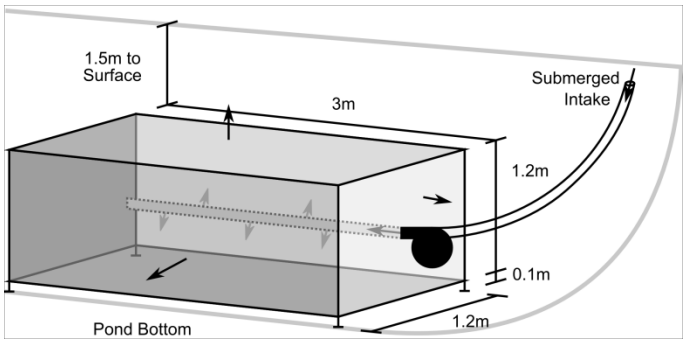

Figure 4-1: Diagram of submerged denitrifying bioreactors for treatment of nitrate in wet detention ponds. Arrows indicate flow paths from intake, through the pump, and radially from the perforated pipe, through the woodchips, and out of the bioreactor. The metal frame was lined with geotextile fabric and secured with cable ties to contain the woodchips.

Bioreactors were placed half-submerged in the pond and filled with a mix of hardwood chips (*Schinus terebinthifolius*). The woodchips were produced locally within a month before installation and were not rinsed. This occurred over the course of two days to allow the chips to saturate and sink before more woodchips were added on top. Bioreactors were then pulled into the pond and then fully submerged. The bioreactors floated for several minutes as the air escaped, and then sank to the pond bottom at least 1.5 m below the surface. The distributor pipes were connected to pumps pulling pond water from an intake approximately 10 m from the bioreactors (Figure 4-2). The flow rate was 20 L min^{-1}, resulting in a theoretical average residence time of 2.3 hours. We calculated the hypothetical time to treat all the water in the pond as well as the time to treat the portion represented by the sampling transects, referred to as the sampling area (Table 4-1). The sampling area accounts for 18% of Pond A and 35% of Pond B (Figure 4-2).

Figure 4-2: Aerial photographs of (a) Pond A and (b) Pond B. The stars and circles indicate approximate locations of the submerged bioreactors and intakes, respectively. The yellow lines show approximate magnitude and direction of sampling transects. The light blue area shows the portion of the pond that transects are assumed to accurately represent. This is referred to as the sampling area and accounts for 18% of Pond A and 35% of Pond B.

Table 4-1: Comparison of ponds with bioreactor installations.

Pond		A	B
Selection Characteristics			
Watershed Area[a]	(ha)	16.4	22.9
Pond Area[a]	(ha)	3.2	2.5
Sampling Area	(ha)	0.56	0.59
Initial NO_3^--N	(mg L^{-1})	7.0 ± 0.7[b]	4.3 ± 0.2[b]
Initial chlorophyll-a	(µg L^{-1})	39 ± 8[c]	40 ± 11[c]
Dates			
Bioreactor Install		11/01/2013	10/26/2013
Pump Start		11/02/2013	11/05/2013
Final Sampling		11/28/2014	11/28/2014
Treatment Time			
Sampling Area	(d)	210	221
Entire Pond Area	(yr)	3.3	2.6

[a]Physical analytes are representative of wet detention ponds in suburban areas in Florida.
[b]Nitrate (NO_3^--N) concentration exceeds West Central Florida recommendation of 1.65 mg L^{-1} (Florida DEP 2015).
[c]Chlorophyll-a level exceeds Florida DEP recommendation of 20 µg L^{-1} for West Central Florida (2015).

Sample Collection and Analysis

Sampling consisted of one pre-installation evaluation and seven post-installation events. Two 100 m sampling transects extended from the bioreactor site to quantify spatial changes in NO_3^- concentrations as the bioreactors cycled the pond water. Samples were collected from a boat approximately 5 m from the bank at points 0, 5, 15, 30, 50, and 100 m from the bioreactor along two transects radiating in semi-opposing directions. Capped polyethylene sample bottles were lowered 10 cm below the surface and then opened to avoid sampling of floating algae. Samples were immediately filtered using 0.45 µm filters and both filters and filtrate were stored on ice in the field. Filters were stored at -20°C and filtered water was refrigerated until analysis within 3 days of collection.

Four analytes were used to quantify water quality before and after bioreactor

installation. The water was analyzed for nitrate plus nitrite nitrogen (NO_3^--N) and sulfate (SO_4^{2-}) using a Dionex ICS-2000 Ion Chromatograph with detention limits of 0.05 mg N L^{-1} and 0.05 mg S L^{-1}, respectively, according to EPA Method 300.0-2.1 (Pfaff 1993). Dissolved organic carbon (DOC) was analyzed with an OI Analytical Total Carbon Analyzer Model 1010 using EPA Method 415.3, and had a detection limit of 0.1 mg DOC L^{-1} (Potter and Wimsatt 2009). Chlorophyll-a was analyzed by spectrophotometry based on the EPA Method 446.0-1 by Arar (1997). Samples from November 2014 were also spectrophotometrically analyzed for ammonium (NH_4^+) (Bower and Holm-Hansen 1980) to corroborate NO_3^- removal via denitrification as opposed to via dissimilatory NO_3^- reduction to NH_4^+. Most of the water samples were analyzed within the recommended 48 hour holding time. Results from samples analyzed within 72 hours showed similar analyte concentrations and were included in further analysis. Concentrations below detection limit were assumed to be equal to the detection limit divided by two.

Software, R version 3.2.1, was used for statistical analysis. Transects were compared with paired t-tests for each analyte. Paired samples from the transects were treated as replicates and averaged into a single data point for further statistical tests. Linear models were used to separately compare concentrations of each analyte to distance from the bioreactor and time since installation. Data were then binned based on natural breaks in pond physiology occurring roughly 20 m from the bioreactor at each pond. Concentrations for each of the analytes were non-normal, based on Shapiro-Wilk tests. Kruskal-Wallis tests were used to determine significant difference with Dunn's tests *post-hoc* (Dunn 1964). Ammonium (NH_4^+) data was only collected

for one sample event. This was used as anecdotal evidence of NO_3^- reduction via denitrification as opposed to dissimilatory NO_3^- reduction to NH_4^+. This was not analyzed statistically.

Results

In both ponds, NO_3^--N dropped below 0.5 mg N L^{-1} along the entire transect within three weeks and remained low for the remainder of the study (Figure 4-3a). Chlorophyll-a (Figure 4-3b) and SO_4^{2-} (Figure 4-3c) were also significantly reduced in both ponds, with chl-a concentrations below the recommended limit of 20 μg L^{-1} (Florida DEP, 2015). Dissolved organic carbon showed a significant increase after bioreactor installation (Figure 4-3d). There were no significant differences between samples within 20 m and greater than 20 m for any analyte. Average NH_4^+ concentrations for samples collected at the end of the study were 0.03 and 0.02 mg N L^{-1} for Ponds A and B.

For each pond and analyte, concentrations were not significantly different within or between transects, suggesting a well-mixed system. Linear models fitting concentrations of each analyte to distance from the bioreactor were not significant (Figure 4-4a-d, Table 4-2). Models comparing each analyte to sampling date were all highly significant (Table 4-2). When pre-installation samples were removed, only chl-a remained significant (Figure 4-4e-h, Table 4-2).

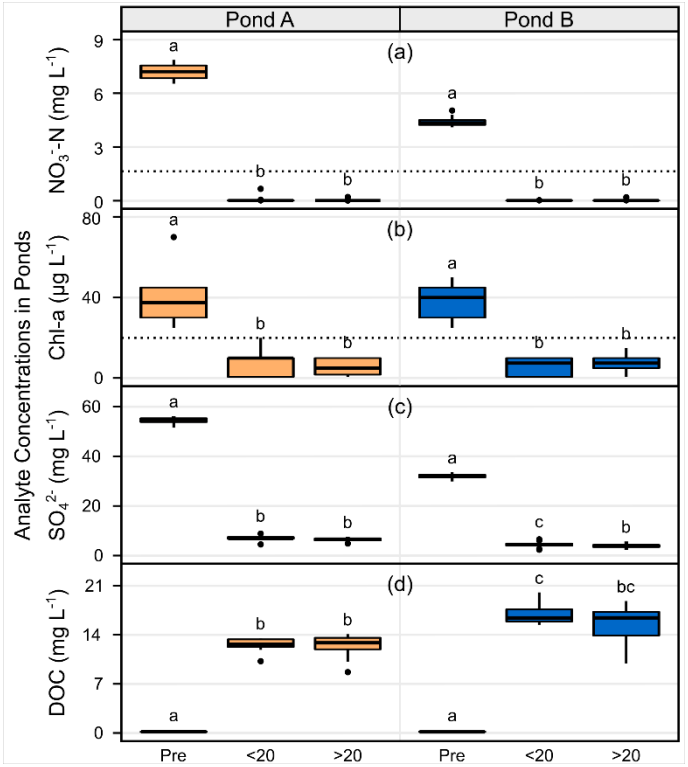

Figure 4-3: Concentrations of analytes in Ponds A and B, measured before bioreactor installation (Pre) and post-installation within 20m of the bioreactor (<20) and beyond 20m (>20). Dotted lines show levels recommended for West Central Florida by the Florida Department of Environmental Protection. Letters indicate significant difference in concentration between groups compared at both ponds (α=0.05).

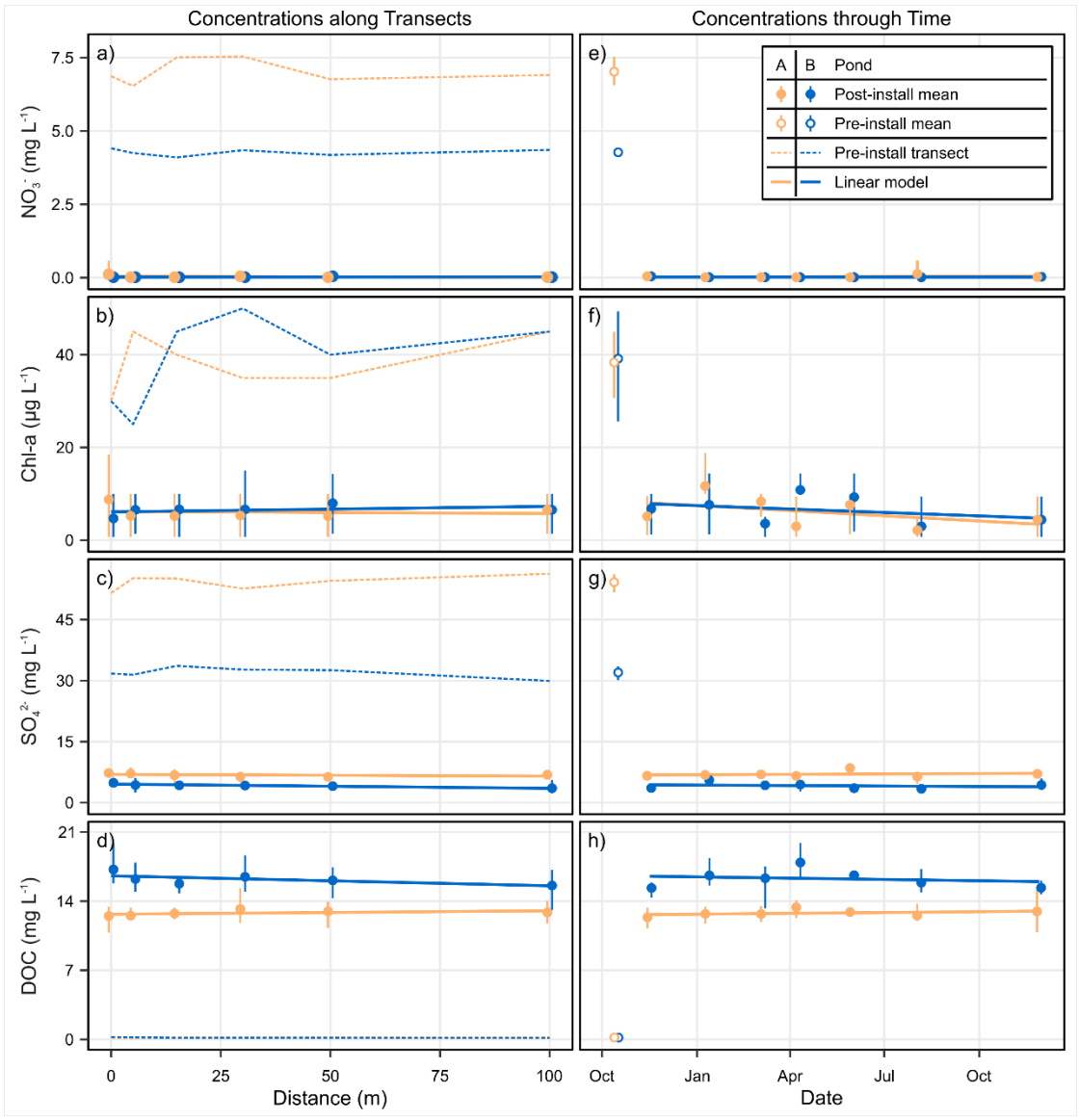

Figure 4-4: Water quality parameters plotted against distance along the transect averaging the entire sampling period (a-d) and plotted by sampling date averaging all samples on the transect (e-h). Points have been shifted slightly to avoid overlap. Error bars indicate the lower and upper 95% confidence intervals of the mean. Dotted lines and hollow points show data from the pre-installation transect sampling in October 2013. Solid lines show the linear models for each pond as shown in Table 4-2. Chlorophyll-a decrease through time (f) was the only significant slope.

Table 4-2: Significance values of slope terms in linear models comparing water quality parameters with distance and time.

Linear Model	p-value[a]	Figure 4-4 ref[b]
Distance LM, excluding pre-install sampling		
NO3 ~Distance + Pond	0.46	a
Chl ~Distance + Pond	0.81	b
DOC ~Distance + Pond	0.40	c
SO4 ~Distance + Pond	0.02*	d
NH4 ~Distance + Pond	0.51	-
Time LM, including pre-install sampling		
NO3 ~Date + Pond	2.5 e-6*	-
Chl ~Date + Pond	8.4 e-9*	-
DOC ~Date + Pond	3.1 e-6*	-
SO4 ~Date + Pond	2.3 e-6*	-
Time LM, excluding pre-install sampling		
NO3 ~Date + Pond	0.63	e
Chl ~Date + Pond	0.01*	f
DOC ~Date + Pond	0.77	g
SO4 ~Date + Pond	0.80	h

*Value significant at the alpha=0.05 threshold.
[a]p-value for the distance or date term in the respective linear model.
[b]Reference to the corresponding facet in Figure 4-4.

Discussion

Evidence of Denitrification

Concentrations of NO_3^- and chl-a were significantly reduced (p-value<0.001) after bioreactor installation in both wet detention ponds as hypothesized. The results of this study are highly dependent upon initial sampling concentrations. While these were similar to samples taken before the study in August 2013, there was possibly a natural change in NO_3^- concentration during the dry season, which generally runs October to May. If NO_3^- concentrations fell between sampling in October and installation of the bioreactors in November, some natural NO_3^- decrease would have been attributed to the bioreactors. However, this is also the beginning of the period

during which Floridians can apply fertilizer to residential areas, which would likely raise NO_3^- concentrations.

Denitrification is only one of several pathways for the reduction of NO_3^-. The significant decrease in chl-a suggests that assimilation is not a major contributor to N reduction in our study. Decreased concentrations of SO_4^{2-} suggest that it is also being biologically reduced and not facilitating NO_3^- reduction through sulfur oxidation. Low NH_4^+ was observed at the end of the study. While this was not measured throughout the study, it provides anecdotal evidence that NO_3^- was not reduced via dissimilatory NO_3^- reduction to NH_4^+. Isotope labeling of NO_3^- and woodchip media would help confirm the internal processes.

Removal Rate Estimates

Removal rate (g N m^{-3} d^{-1}) is the commonly used metric to evaluate and compare efficiency of N treatment in agricultural denitrifying bioreactors (Schipper et al. 2010). This calculates the mass of N removed per time and normalizes it to the volume in which denitrification occurs. In traditional applications of bioreactors, mass of N removed per time is equal to the change in concentration between inflow and outflow NO_3^- multiplied by flow rate. Our design did not have a distinct outlet point and the intake was likely influenced by effluent from the bioreactor. Instead, we approximate the mass of N removed as the difference in concentration between sampling events multiplied by the volume of pond represented by the sample transects. This is divided by the time interval between sampling for the mass removed per time and then normalized by bioreactor volume as before. NO_3^- concentration

dropped too quickly across the entire transect to calculate the rate of spread in low NO_3^- or to calculate more than the RR between the first samples. Estimated initial RRs were 1026 and 470 g N m^{-3} d^{-1} for Pond A and B, respectively. These are larger than the highest average RR of 30 g N m^{-3} d^{-1} reported in agricultural bioreactors (Bell et al., 2015). These are also higher than bioreactors used to treat aquaculture, where consistent flow rates are more comparable to our design (von Ahnen et al. 2016).

These rates are normalized by bioreactor pore volume, which allows for comparison between bioreactors of different sizes, including lab-scale and field-scale. This is an appropriate measure for conventional bioreactors with defined inflow and outflow points and a contained volume, as described by Schipper, et al. (2010). While the media is contained in the submerged bioreactors, the boundaries for denitrification to occur are not as clear. DOC increased in the ponds after installation, with pond concentrations similar to agricultural bioreactor effluent (Hassanpour et al. 2017). Concentrations increased along the entire length of sampling transects, likely aided by particulate carbon and sawdust in the woodchips (Rambags et al. 2016) and disturbance in the pond from installation. The alleviation of a DOC limitation could encourage denitrification beyond the bioreactor. Evidence from wetland soils show rapid activation of denitrification when the right conditions occur (Zhi and Ji 2014) and a number of studies have documented high rates of denitrification in the top 10 cm of soil and pond sediment (Hill 1995; Li et al., 2010; Brauer et al., 2015). If we assume that high DOC activated denitrification in 10 cm of pond sediment in the entire sampling area in addition to the bioreactor volume, RR is 7.9 and 3.4 g N m^{-3} d^{-1} in Pond A and B, respectively.

Extensions

The narrow locations within the ponds where the bioreactors were located potentially limited pumps mixing water from the entire pond. However, samples collected greater than 20 m from the bioreactors extended well into open portions of the pond and NO_3^- was not significantly higher than within 20 m ($p=0.32$). This suggests that water quality impacts and mixing were not limited to the portion closest to the bioreactor. Instead, the extent of water quality benefits may not be fully recognized because of our assumption that treatment was confined to the sampling area. In addition, measurements of NO_3^- concentration at the pump intake would allow for calculation of RR that is more similar comparison to agricultural bioreactor calculations.

Further work is necessary to verify these results in other wet detention ponds and climates. Our experimental design can be substantially improved by including control or "paired" ponds instead of relying solely on a before-after sampling approach. High RRs and elevated DOC suggest carbon is leaching from the bioreactors, which may shorten media life. Long-term monitoring is necessary to determine if this is indeed the case and will be invaluable in predicting when media is consumed and a drop in efficiency may occur. We also suggest additional sampling at a higher temporal resolution immediately after the bioreactor is installed and sampling transects that cover the entire pond area to improve RR estimates. Analysis of nitrous oxide and methane emissions from the pond surface would quantify the ratio of complete denitrification and the potential greenhouse gas impacts of reducing conditions in the pond. If denitrification is occurring outside of the bioreactor, the large structure and

pumping may be unnecessary. Instead, large-scale denitrification may be achievable with woodchips dispersed throughout the pond.

Conclusion

This was a case study with few replicates and limited transect length and study period. Based on the data collected, the two pond bioreactors successfully reduced NO_3^- concentrations below 2 mg N L^{-1}, probably via denitrification in the entire sampling area. Analysis of other indicators, including chl-a, SO_4^{2-}, and NH_4^+, supports this conclusion. The low NO_3^- and chl-a concentrations suggest that bioreactors may be a potential alternative to chemical herbicides in addition to providing efficient nutrient treatment. The rapid rate of removal and the mixing throughout the entire sampling transects did not allow us to model the progress of NO_3^- reduction throughout the ponds. Because of this, RRs were conservative estimates of what may have been more extensive. This study shows the potential for denitrifying bioreactors, which have been successfully implemented to treat NO_3^- in agricultural runoff, to be applied to suburban systems for water quality improvement and management. The ubiquity of wet detention ponds throughout suburban areas make them an ideal candidate for bioreactor installations to reduce N pollution to waterbodies. A simple retrofit, like the one described in this study, could significantly reduce the footprint of society on the N cycle close to the source and benefit estuarine and coastal waters.

REFERENCES

Addy, K., Gold, A. J., Christianson, L. E., David, M. B., Schipper, L. A., and Ratigan, N. A. (2016). "Denitrifying bioreactors for nitrate removal: A meta-analysis." *Journal of Environmental Quality*, 45(3), 873–881.

Arar, E. J. (1997). "In vitro determination of chlorophylls a, b, c1 + c2 and pheopigments in marine and freshwater algae by visible spectrophotometry." *Method 446.0-1*, U. S. Environmental Protection Agency, Cincinnati, OH.

Bell, N. L., Cooke, R. A. C., Olsen, T., David, M. B., and Hudson, R. (2015). "Characterizing the performance of denitrifying bioreactors during simulated subsurface drainage events." *Journal of Environmental Quality*, 44(5), 1647–1656.

Bettez, N. D., and Groffman, P. M. (2012). "Denitrification potential in stormwater control structures and natural riparian zones in an urban landscape." *Environmental Science & Technology*, 46(20), 10909–10917.

Borne, K. E., Tanner, C. C., and Fassman-Beck, E. A. (2013). "Stormwater nitrogen removal performance of a floating treatment wetland." *Water Science and Technology*, 68(7), 1657–1664.

Bower, C. E., and Holm-Hansen, T. (1980). "A Salicylate–Hypochlorite Method for Determining Ammonia in Seawater." *Canadian Journal of Fisheries and Aquatic Sciences*, 37(5), 794–798.

Brauer, N., Maynard, J.J., Dahlgren, R.A, and O'Geen, A.T. (2015). "Fate of nitrate in seepage from a restord wetland receiving agricultural tailwater." *Ecological Engineering*, 81, 207–217.

Carpenter, S. R., Caraco, N. F., Correll, D. L., Howarth, R. W., Sharpley, A. N., and Smith, V. H. (1998). "Nonpoint pollution of surface waters with phosphorus and nitrogen." *Ecological Applications*, 8(3), 559–568.

Collins, K. A., Lawrence, T. J., Stander, E. K., Jontos, R. J., Kaushal, S. S., Newcomer, T. A., Grimm, N. B., and Cole Ekberg, M. L. (2010). "Opportunities and challenges for managing nitrogen in urban stormwater: A review and synthesis." *Ecological Engineering*, 36(11), 1507–1519.

Dunn, O. J. (1964). "Multiple comparisons using rank sums." *Technometrics*, 6(3), 241–252.

Florida Department of Environmental Protection (DEP). (2015). "Surface water quality standards." *Chapter 62-302*, Florida Department of Environmental Protection, Pensacola, FL.

Hassanpour, B., Giri, S., Pluer, W.T., Steenhuis, T.S., and Geohring, L.D. (2017). "Seasonal performance of denitrifying bioreactors in the Northeastern United States: Field trials." *Journal of Environmental Management*, 202, 242–253.

Hill, A., (1996). "Nitrate removal in stream riparian zones." *Journal of Environmental Quality*, 25, 743–755.

Kemp, W. M., Boynton, W. R., Adolf, J. E., Boesch, D. F., Boicourt, W. C., Brush, G. S., Cornwell, J. C., Fisher, T. R., Glibert, P. M., Hagy, J. D., Harding, L. W., Houde, E. D., Kimmel, D. G., Miller, W. D., Newell, R. I. E., Roman, M. R., Smith, E. M., and Stevenson, J. C. (2005). "Eutrophication of Chesapeake Bay: historical trends and ecological interactions." *Marine Ecology Progress Series*, 303, 1–29.

Li, F., Yang, R., Ti, C., Lang, M., Kimura, S.D., and Yan, X. (2010). "Denitrification characteristics of pond sediments in a Chinese agricultural watershed." *Soil Science and Plant Nutrition*, 56(1), 66–71.

Li, L., and Davis, A. P. (2014). "Urban stormwater runoff nitrogen composition and fate in bioretention systems." *Environmental Science & Technology*, 48(6), 3403–3410.

Lovett, G. M., Traynor, M. M., Pouyat, R. V., Carreiro, M. M., Zhu, W. X., and Baxter, J. W. (2000). "Atmospheric deposition to oak forests along an urban-rural gradient." *Environmental Science and Technology*, 34(20), 4294–4300.

Lucke, T., and Nichols, P. W. B. (2015). "The pollution removal and stormwater reduction performance of street-side bioretention basins after ten years in operation." *Science of the Total Environment*, Elsevier B.V., 536, 784–792.

Mallin, M. A., Ensign, S. H., Wheeler, T. L., and Mayes, D. B. (1998). "Pollutant removal efficacy of three wet detention ponds." *Journal of Environmental Quality*, 31(2), 654–660.

Morse, N. R., McPhillips, L. E., Shapleigh, J. P., and Walter, M. T. (2017). "The Role of Denitrification in Stormwater Detention Basin Treatment of Nitrogen." *Environmental Science and Technology*, 51(14), 7928–7935.

Osmond, D. L., and Hardy, D. H. (2004). "Characterization of turf practices in five North Carolina communities." *Journal of Environmental Quality*, 33(2), 565–575.

Pfaff, J. D. (1993). "Determination of inorganic anions by ion chromatography." *Method 300.0-2.1*, U. S. Environmental Protection Agency, Cincinnati, OH.

Potter, B. B., and Wimsatt, J. C. (2009). "Determination of total organic carbon and specific UV absorbance at 254 nm in source water and drinking water." *Method 415.3*, U. S. Environmental Protection Agency, Cincinnati, OH.

Rambags, F., Tanner, C. C., Stott, R. and Schipper, L A. (2016). "Fecal bacteria, bacteriophage, and nutrient reductions in a full-scale denitrifying woodchip bioreactor." *Journal of Environmental Quality*, 45(3), 847–854.

Schipper, L. A., Robertson, W. D., Gold, A. J., Jaynes, D. B., and Cameron, S. C. (2010). "Denitrifying bioreactors—An approach for reducing nitrate loads to receiving waters." *Ecological Engineering*, 36(11), 1532–1543.

Schwartz, D., Sample, D. J., and Grizzard, T. J. (2017). "Evaluating the performance of a retrofitted stormwater wet pond for treatment of urban runoff." *Environmental Monitoring and Assessment*, Environmental Monitoring and Assessment, 189(6).

von Ahnen, M., Pedersen, P.B., Hoffmann, C.C., Dalsgaard, J., 2016. Optimizing nitrate removal in woodchip beds treating aquaculture effluents. *Aquaculture*, 458, 47–54.

Winston, R. J., Hunt, W. F., and Pluer, W. T. (2017). "Nutrient and sediment reduction through upflow filtration of stormwater retention pond effluent." *Journal of Environmental Engineering*, 143(5), 1–8.

Zhi, W., and Ji, G. (2014). "Quantitative response relationships between nitrogen transformation rates and nitrogen functional genes in a tidal flow constructed wetland under C/N ratio constraints." *Water Research*, 64, 32–41.

CHAPTER 5

DENITRIFYING BIOREACTORS FOR ENHANCED NITRATE REDUCDTION IN ROADSIDE DITCHES

Introduction

Excess nitrogen (N) from nonpoint sources is a persistent threat to water quality worldwide. Significant loads from agricultural field runoff and shallow groundwater, as well as suburban runoff contribute to this problem (Shields et al., 2008; Kaushal et al., 2011). The excess N, typically in the form of nitrate (NO_3^-), disrupts aquatic ecosystems, causing eutrophication and hypoxia (Kemp et al., 2005). Microbial denitrification can reduce NO_3^- to dinitrogen gas by respiration of organic matter under anaerobic conditions, a process that occurs naturally in saturated soils and stream sediments (Seitzinger et al., 2006).

Despite the ubiquity of denitrifying microbes, alterations in watershed hydrology can limit opportunities for treatment of NO_3^- pollution. Agricultural and roadside ditches channelize flow throughout the landscape and move it quickly to surface water. Buchanan et al. (2013) found that more than 30% of the water leaving a watershed passes through a roadside ditch. This decreases time water spends in soils where NO_3^- can potentially be reduced. McPhillips et al. (2016) found that denitrification occurs at higher rates in ditches compared with surrounding land. However, residence time of water ditches is generally lower than in un-manipulated landscapes, which results in a net decrease in NO_3^- removal in some cases.

The frequency of saturation in ditches suggests that these could be ideal denitrification hotspots with some engineered enhancements. Wetlands (Hanson et al.,

1994), riparian buffers (Bettez and Groffman, 2012), and stream sediments (Beaulieu et al., 2011) have higher *in-situ* rates of denitrification than ditches. Ditch management focuses on water quantity and ditches are routinely scraped to maximize transport capacity. This leaves little topsoil and organic carbon to facilitate infiltration or hyporheic exchange that would transport NO_3^- to anaerobic micropores in the soil (Harvey et al., 2013).

Denitrifying bioreactors have proven effective in treating NO_3^- in agricultural tile drainage (e.g. Schipper et al., 2010). Tile drains limit soil contact and residence time similar to ditches. The bioreactors route drainage through a bed of saturated woodchips that provide ideal conditions for denitrification (Schipper et al., 2010). The results are even higher than natural analogs, with removal rate (RR), a metric of removed NO_3^- load scaled by bioreactor volume, up to 30 g N m^{-3} d^{-1} (Bell, et al. 2016).

Several studies have explored the application of bioreactors beyond agricultural tile drainage with positive results (Elgood et al., 2010; Tanner et al., 2012; Lepine et al., 2016). While typical bioreactor designs are subsurface, internal measurements of dissolved oxygen show inflow reaches anoxic conditions quickly (Healy et al., 2015). This may allow bioreactors to be installed above ground without reducing critically volume within the bioreactor suitable for denitrification. In this study, a bioreactor was designed for installment into a roadside ditch receiving agricultural runoff with high NO_3^- concentrations to assess the feasibility of using roadside ditches as opportunities to treat concentrated flows on nonpoint source pollution.

Methods

Ditch Bioreactor Design

A ditch reach was selected just downstream of a monitoring site in Tompkins County, New York State. The ditch drains approximately 40 ha of agricultural fields of shallow silt loam soils. Two years of prior monitoring of the site showed excess NO_3^- concentrations, moderate rates of *in-situ* denitrification, and intermittent flow (Schneider and Marino, 2015). The design for the ditch bioreactor was based on established procedures for agricultural denitrifying bioreactors. Several adjustments were required to modify the bioreactor for features of the ditch. The bioreactor was sized to span the entire ditch width and a depth to contain baseflow using natural ditch slope (approximate hydraulic gradient) and hydraulic conductivity of the *Fraxinus sp.* woodchips. The dimensions of the bioreactor were 5 m long by 1 m wide by 10 cm high. This design produced a theoretical average hydraulic retention time of 1.2 hr when flow depth is equal to bioreactor height. In May 2016, the bioreactor was installed on the surface of the cleared ditch bottom. The woodchips were contained in a cloth netting with holes approximately 0.8 cm x 0.8 cm openings and cinched closed with cable ties forming a highly permeable, woodchip-filled mattress. This was secured in place with rebar driven through the bioreactor and deep into the ditch bottom (Figure 5-1).

Figure 5-1: Ditch bioreactor right after installation. A cloth netting contained the woodchips and four rebar stakes secured the bioreactor during high flow rates and helped maintain its shape.

Bioreactor Monitoring

HOBO pressure transducers were installed just upstream of the bioreactor and outside of the ditch to record hourly air and water temperature and pressure in the ditch. Two ISCO 6712 autosamplers, fitted with water level actuators, were installed at the site to monitor directly upstream and downstream of the bioreactor during the 2016 and 2017 growing seasons. The actuators triggered ISCO sampling when water levels in the ditch increased. Upstream and downstream actuators were adjusted weekly to be 0.5 cm above the current water level. This initiated sampling for upstream and downstream as close together as possible and limited ISCO sampling to storm events.

Samplers were programmed to collect 200 mL samples at initiation and every 30 minutes afterwards, compositing 4 samples per bottle until all 24 bottles were full. This provided a two-hour sampling resolution for 48 hours during and after stormflows. Bottles were pre-acidified to preserve NO_3^- concentration and samples

were filtered and refrigerated at 4°C within 72 hours of collection. Weekly grab samples were collected upstream and downstream of the bioreactor throughout the monitoring period to compare bioreactor performance during baseflow design conditions with storms. These grab samples of baseflow were processed similarly to the storm samples for consistency. Samples were analyzed colorimetrically for combined nitrate-nitrite nitrogen (NO_3^--N) (O'Dell, 1993) and ammonium (NH_4^+) (Bower and Holm-Hansen, 1980). Additionally, some non-acidified grab samples were analyzed for total phosphorous using an Inductively Coupled Plasma Spectrometer using EPA Method 200.7 (Martin, T.D., Brockhoff, C.A., Creed, 1994).

Statistical Analysis

The R software environment version 3.2.1 was used for data processing and statistical analyses. Flows were calculated using a rating curve developed from twelve flow measurements taken periodically throughout the monitoring period. Gaps in flow data were filled using data from a nearby USGS gage station (0423401815). Gage station flow data was scaled based on the last day of measurement before the gap and first day the instruments were reinstalled. Due to the short length of the bioreactor, we assumed that flow remained constant along the ditch length. NO_3^- concentration data for each sampling flow condition were compiled with corresponding flow depth and temperature data. Storm event data were summarized using flow-weighted average upstream and downstream NO_3^- concentrations and average flow for each event. Based on flow depth, we also calculated the portion of flow expected to pass through the bioreactor and the portion expected to flow above the bioreactor. While these two

flowpaths are not discrete, this separation provides a rough estimate of percent flow with sufficient retention time for treatment.

RR is the commonly used metric of denitrification in bioreactors. However, the bioreactor in this study was significantly smaller and designed with a different methodology than agricultural bioreactors. Therefore, we use RR, as described by Schipper et al. (2010) as well as removal efficiency (RE), as described by Lepine et al. (2016), to evaluate bioreactor performance. RE does not include bioreactor volume, providing a complementary perspective on NO_3^- removal. Since there were no flow control structures that provided defined inflow and outflow points for the ditch bioreactor, measurements upstream and downstream of the ditch bioreactor were used for concentration differences. Flow, RR, and NO_3^- concentrations were log-transformed for normality. RE displayed a uniform distribution and was kept untransformed for further analyses. All tests used a significance level of $\alpha=0.05$. One-sample Student t-tests and Wilcoxon signed rank tests were used to determine if RR and RE, respectively, were significantly greater than zero for each flow condition. Additionally, RR and RE were compared between flow conditions using a 2-sample t-test and Wilcoxon rank sum test, respectively. A multiple linear regression was used to determine significant predictors of RR among variables of flow rate, flow through the bioreactor (a portion of flow rate), flow condition (whether baseflow or stormflow), and upstream NO_3^- concentration. Plots of quantiles and residuals verified that transformed data satisfied assumptions for linear regression. Due to non-normality and zero values that prevented log-transformation, a Wilcoxon rank sum test was used to analyze phosphorous concentrations upstream and downstream of the bioreactor.

Results and Discussion

Observed Nitrate Treatment

During two growing seasons, 49 grab samples were collected and 12 storms were monitored. Flow, NO_3^- concentrations, RR and RE are shown in Figure 5-2. Downstream NO_3^- was significantly less than upstream NO_3^- during both baseflow and stormflow sampling. The ditch bioreactor experienced a wide range of flows, inflow NO_3^- concentrations, and temperature that resulted in a wide range of performance. The first year of monitoring, 2016, was a drought year with 39% less rainfall during the growing season compared to annual averages while 2017 was slightly above average. Air temperature experienced by the ditch bioreactor had a wider range and was more variable compared with bioreactors treating agricultural tile drainage in similar soil and climate (Hassanpour et al., 2017). Flow was flashy in comparison with agricultural bioreactors, which is characteristic of roadside ditches.

Despite variable conditions, several instances of RR were orders of magnitude higher than the maximum of 30 g N m^{-3} d^{-1} previously observed in tile drain systems (Bell et al., 2015). This is caused by the small size of the bioreactor and the relatively high flow rates it received, both of which are used in calculating RR. Previous work by Addy et al. (2016) showed that low inflow NO_3^- concentrations limit denitrification in bioreactors. Their threshold of 2 mg N L^{-1} was applied to our dataset. This removed nine samples from further analysis. RR and RE varied during both years and were not significantly different between 2016 and 2017. However, the storm samples had a significantly higher average RR than the grab samples of baseflow conditions (Figure

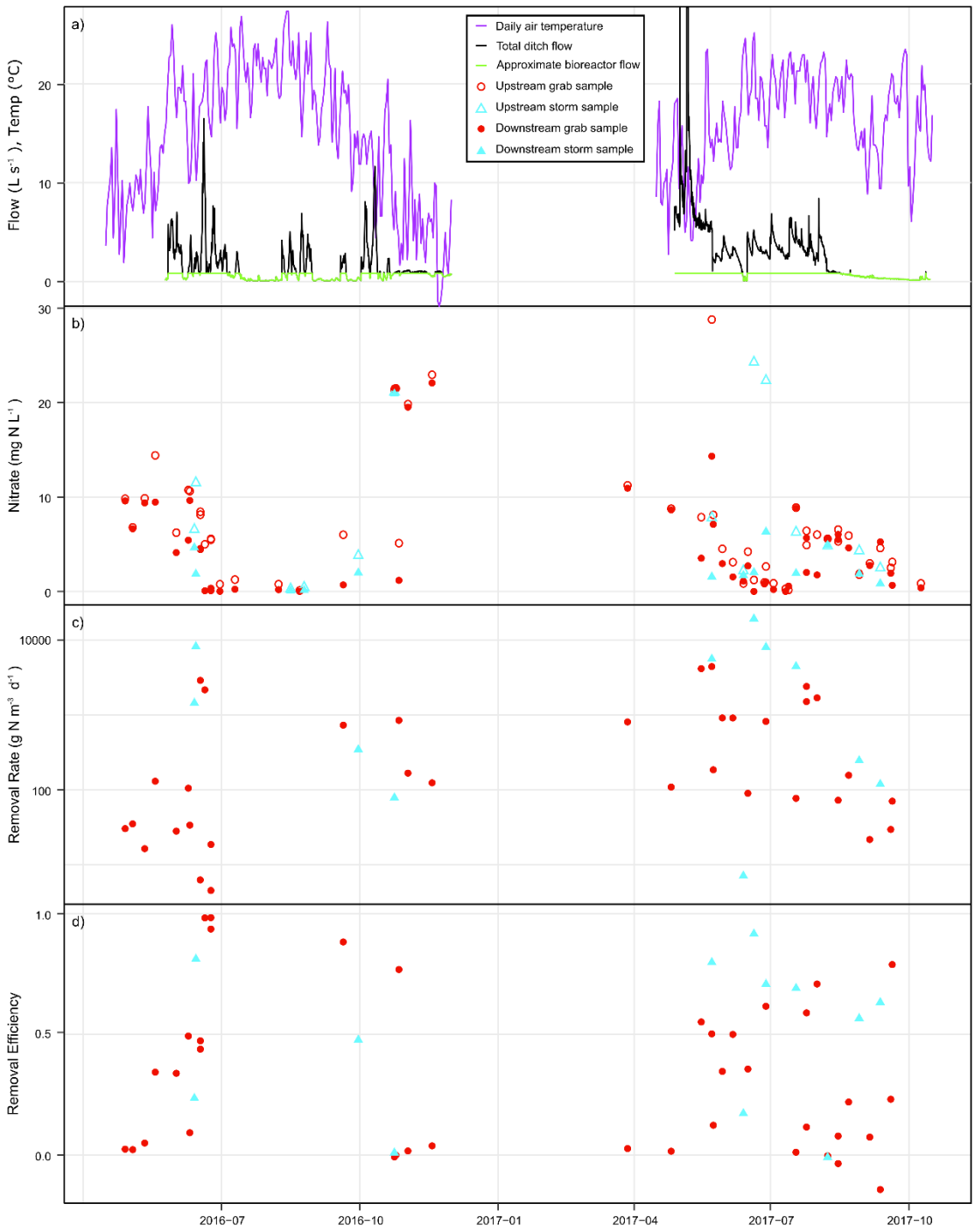

Figure 5-2: Temperature and flow (a), upstream and downstream NO_3^- concentrations (b), removal rate (RR) (c), and removal efficiency (RE) (d) in the ditch bioreactor during the 2016 and 2017 growing seasons. The black flow line indicates total flow in the ditch and the green line represents approximate flow through the ditch bioreactor. Point color and shape indicate the sampling flow conditions, whether baseflow (red circles) or flow-weighted averages from storm sampling (blue triangles), and fill indicates upstream (white) and downstream (colored) sample locations.

5-3a). RE was also higher during storm events though the difference was not significant (p=0.18) (Figure 5-3d).

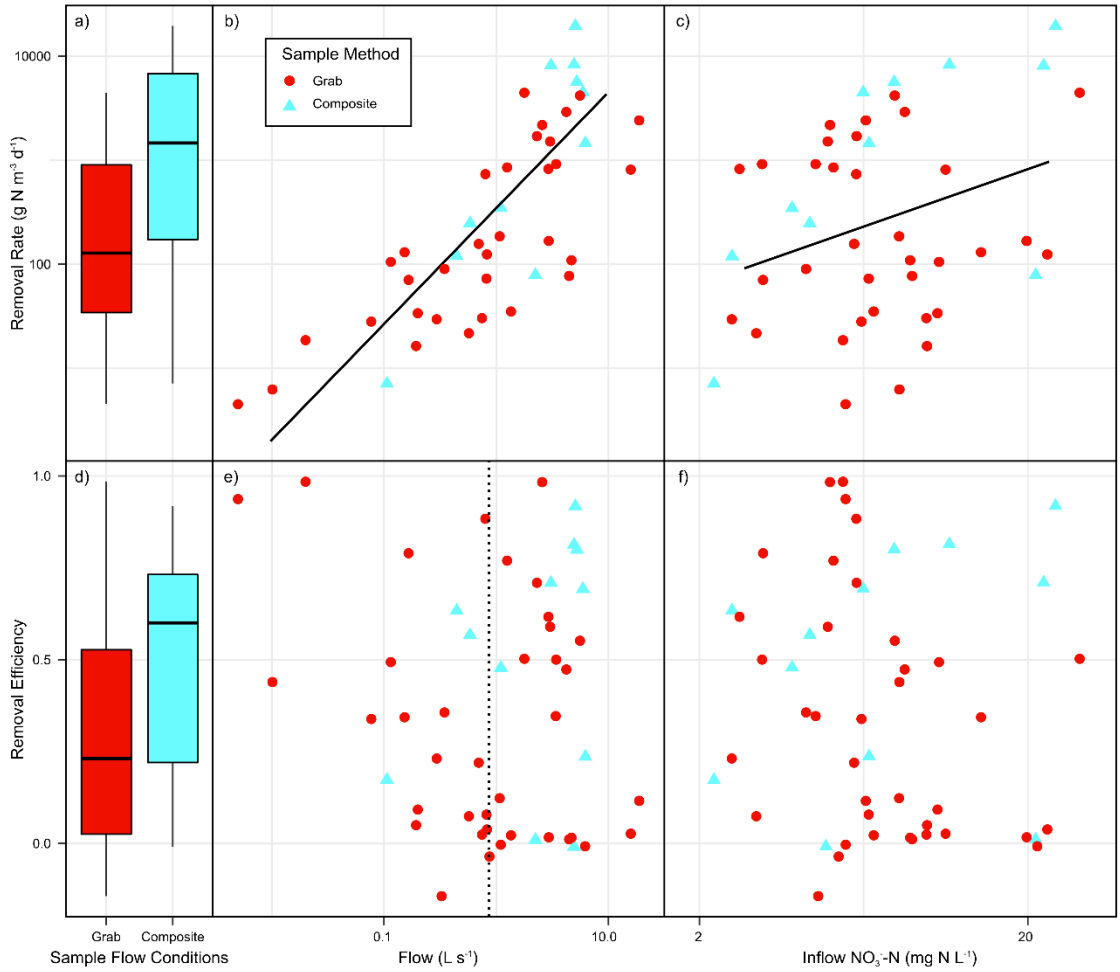

Figure 5-3: Log transformed values of removal rate (RR) (a-c) and untransformed removal efficiency (RE) (d-f) of NO_3^- separated by sampling flow method and plotted against log-transformed flow rate and log-transformed upstream nitrate concentrations. Point color and shape indicate the sampling flow conditions, whether baseflow (red circles) or flow-weighted averages from storm sampling (blue triangles). Solid lines present linear models while the dotted line shows an observed threshold in the plot of RE and flow at around 0.1 L s^{-1}.

Other Nutrient Pollutants

Ammonium remained low during the monitoring period, never exceeding concentrations of 0.05 mg N L^{-1}. Due to the low NH_4^+ concentrations, especially relative to high NO_3^- concentrations, NH_4^+ is not considered a significant contributor

to inorganic N in ditchwater. Measurements of nitrous oxide, an intermediate product of denitrification, are necessary to both verify NO3- removal is via denitrification and that the process is general carrying to completion. Incomplete denitrification would result in higher nitrous oxide emissions, producing a potent greenhouse gas.

Similarly, total phosphorus concentrations were low throughout the two-year monitoring period. Twelve of the 44 samples (22 each of upstream and downstream grab samples) had values below the instrument detection limit (50 µg L^{-1}). While the downstream concentration was significantly higher than upstream, the difference was generally small (~5 µg L^{-1} on average). Most concentration increases occurred during low flow conditions. This may be due to leaching of phosphorus from the woodchips as observed in field bioreactors by Pluer et al. (2016). The small concentration increases that occurred mostly during low flow conditions did not an overall significant increase in phosphorus load downstream of the bioreactor.

Scaling Annual Removal Rate

The multiple linear regression indicated that total flow was a significant variable influencing RR ($p<0.005$). Figure 5-3b shows a linear model fitting log-transformed values of RR against log-transformed flow rate. This model was significant for flow ($p<1x10^{-9}$) and fit RR well ($R^2=0.61$). No significant linear relationship existed between RE and log-transformed flow rate (Figure 5-3e). However, there appears to be a threshold of flow above which RE can be very low. On the plot, this is at approximately 0.1 L s^{-1}. Based on flow depth, flow passes over the

bioreactor at 0.86 L s^{-1} so this threshold occurs at depths much lower than overtopping the ditch bioreactor.

Upstream NO_3^- concentration was not a significant variable in the multiple linear regression of RR. A single-variable linear fit for this was not as significant as it was for flow and fit the data poorly ($p=0.07$, $R^2=0.05$, Figure 5-3c). There was no apparent relationship between log-transformed upstream NO_3^- concentration and RE either (Figure 5-3f). There was also no significant relationship between RR and RE (Figure 5-4). Together, these factors indicate that high RR is driven more by flow than NO_3^- concentration reduction.

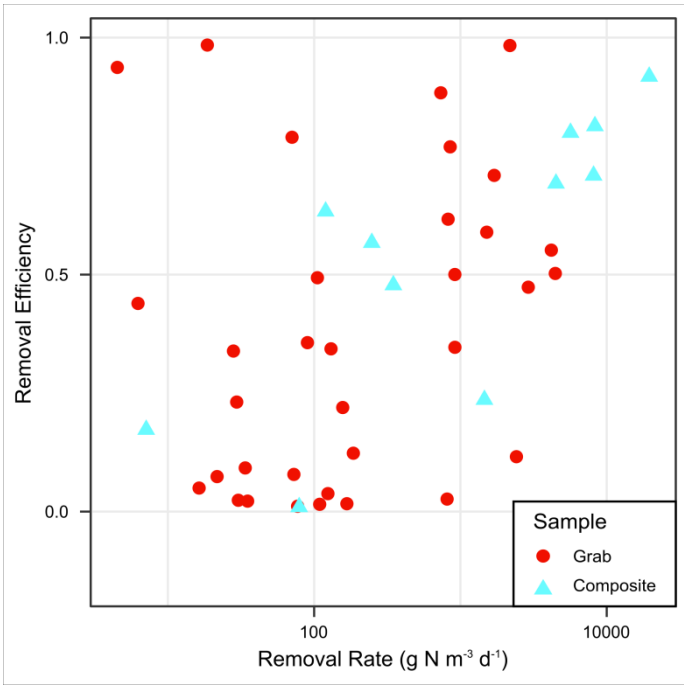

Figure 5-4: Untransformed removal efficiency plotted against log transformed values of removal rate (RR). Point color and shape indicate the sampling flow conditions, whether baseflow (red circles) or flow-weighted averages from storm sampling (blue triangles). There were no trends between the two metrics.

Continuous monitoring of NO_3^- concentration is more difficult and expensive than for flow depth. While models that include NO_3^- concentration would be better

predictors of actual RR, it is difficult to obtain or estimate this information to apply the model. Furthermore, flow will vary over a much wider range than NO_3^- concentrations. For this reason, we limited our model of RR to include only flow rate. This model explained the majority of variation in RR and is therefore a strong predictor of what we expect to occur in the ditch bioreactor between sampling events. Applying this model to our continuous flow data, the average RR is 655 g N m^{-3} d^{-1}. This suggests that this small bioreactor in the roadside ditch could remove 120 kg N, annually. Assuming that these rates would only apply to the growing season, the bioreactor would remove 40 kg N annually.

Conclusions

This study found that a small denitrifying bioreactor installed above ground in the bottom of a roadside ditch was able to achieve persistent and significant reductions in NO_3^- load. In this design, water passively flows through and over a contained woodchip mattress, which is able to provide organic carbon and anaerobic conditions necessary to increase the rate of denitrification. Downstream samples were significantly lower in NO_3^- concentration than upstream of the bioreactor. Ammonium concentration remained low throughout monitoring and there was a slight, insignificant increase in total phosphorus load. RR was most significantly driven by flow rate in the ditch, which typically exceeded the depth of the bioreactor. A linear regression fitting log-transformed flow to log-transformed RR was used to predict RR for two growing seasons. This resulted in an average annual removal of 120 kg of inorganic N from the ditch water.

This study is limited to a single ditch bioreactor; however, the results are supported by similar findings in bioreactors in agricultural fields (e.g. Addy et al., 2016). While additional sites and flow conditions are necessary before scaling the application of ditch bioreactors to a watershed or larger scales, the results in this study suggest this as a promising new best management practice. It is likely that larger ditch bioreactors could achieve more NO_3^- removal but would also lower RR due to the size scaling. Monitoring during a full year is also necessary to confirm whether high RR is suppressed by low temperatures during spring melt events. Placement of the ditch bioreactor above ground may lead to aerobic conditions during low flows, which would result in accelerated decomposition of the woodchip media. This, along with the small size of the bioreactor, could lead to a reduced lifespan when compared with greater than 20 years of longevity demonstrated in traditional bioreactors (e.g. Long et al., 2011; Robertson et al., 2008). Continued sampling of this ditch bioreactor and other long-term studies are necessary to determine a lifespan of a bioreactor implemented this way. Ditch bioreactors may prove to be a widely applicable and highly effective way to treat NO_3^- throughout the watershed and significantly decrease loads to receiving water bodies.

REFERENCES

Addy, K., Gold, A.J., Christianson, L.E., David, M.B., Schipper, L.A., Ratigan, N.A., 2016. Denitrifying bioreactors for nitrate removal: A meta-analysis. *J. Environ. Qual.* 45, 873–881.

Beaulieu, J.J., Tank, J.L., Hamilton, S.K., Wollheim, W.M., Hall, R.O., Mulholland, P.J., Peterson, B.J., Ashkenas, L.R., Cooper, L.W., Dahm, C.N., Dodds, W.K., Grimm, N.B., Johnson, S.L., McDowell, W.H., Poole, G.C., Valett, H.M., Arango, C.P., Bernot, M.J., Burgin, A.J., Crenshaw, C.L., Helton, A.M., Johnson, L.T., O'Brien, J.M., Potter, J.D., Sheibley, R.W., Sobota, D.J., Thomas, S.M., 2011. Nitrous oxide emission from denitrification in stream and river networks. *Proc. Natl. Acad. Sci.* 108, 214–219.

Bell, N.L., Cooke, R.A.C., Olsen, T., David, M.B., Hudson, R. 2015. Characterizing the performance of denitrifying bioreactors during simulated subsurface drainage events. *J. Environ. Qual.* 44, 1647–1656.

Bettez, N.D., Groffman, P.M., 2012. Denitrification potential in stormwater control structures and natural riparian zones in an urban landscape. *Environ. Sci. Technol.* 46, 10909–10917.

Bower, C.E., Holm-Hansen, T., 1980. A Salicylate–Hypochlorite Method for Determining Ammonia in Seawater. *Can. J. Fish. Aquat. Sci.* 37, 794–798.

Buchanan, B.P., Falbo, K., Schneider, R.L., Easton, Z.M., Walter, M.T., 2013. Hydrological impact of roadside ditches in an agricultural watershed in Central New York: Implications for non-point source pollutant transport. *Hydrol. Process.* 27, 2422–2437.

Elgood, Z., Robertson, W.D., Schiff, S.L., Elgood, R., 2010. Nitrate removal and greenhouse gas production in a stream-bed denitrifying bioreactor. *Ecol. Eng.* 36, 1575–1580.

Hanson, G.C., Groffman, P.M., Gold, A.J., 1994. Denitrification in Riparian Wetlands Receiving High and Low Groundwater Nitrate Inputs. *J. Environ. Qual.* 23, 917.

Harvey, J.W., Böhlke, J.K., Voytek, M.A., Scott, D., Tobias, C.R., 2013. Hyporheic zone denitrification: Controls on effective reaction depth and contribution to whole-stream mass balance. *Water Resour. Res.* 49, 6298–6316.

Hassanpour, B., Giri, S., Pluer, W.T., Steenhuis, T.S., Geohring, L.D., 2017. Seasonal performance of denitrifying bioreactors in the Northeastern United States: Field trials. *J. Environ. Manage*. 202, 242–253.

Healy, M.G., Barrett, M., Lanigan, G.J., João Serrenho, A., Ibrahim, T.G., Thornton, S.F., Rolfe, S.A., Huang, W.E., Fenton, O., 2015. Optimizing nitrate removal and evaluating pollution swapping trade-offs from laboratory denitrification bioreactors. *Ecol. Eng*. 74, 290–301.

Kaushal, S.S., Groffman, P.M., Band, L.E., Elliott, E.M., Shields, C.A., Kendall, C., 2011. Tracking nonpoint source nitrogen pollution in human-impacted watersheds. *Environ. Sci. Technol.* 45, 8225–8232.

Kemp, W.M., Boynton, W.R., Adolf, J.E., Boesch, D.F., Boicourt, W.C., Brush, G.S., Cornwell, J.C., Fisher, T.R., Glibert, P.M., Hagy, J.D., Harding, L.W., Houde, E.D., Kimmel, D.G., Miller, W.D., Newell, R.I.E., Roman, M.R., Smith, E.M., Stevenson, J.C., 2005. Eutrophication of Chesapeake Bay: historical trends and ecological interactions. *Mar. Ecol. Prog. Ser.* 303, 1–29.

Lepine, C., Christianson, L.E., Sharrer, K.L., Summerfelt, S.T., 2016. Optimizing Hydraulic Retention Times in Denitrifying Woodchip Bioreactors Treating Recirculating Aquaculture System Wastewater. *J. Environ. Qual.* 45, 813–821.

Long, L.M., Schipper, L.A., Bruesewitz, D.A., 2011. Long-term nitrate removal in a denitrification wall. *Agric. Ecosyst. Environ.* 140, 514–520.

Martin, T.D., Brockhoff, C.A., Creed, J.T., 1994. Determination of metals and trace elements in water and wastes by inductively coupled plasma-atomic emission spectrometry. *Method 200.7-4.4*.

McPhillips, L.E., Groffman, P.M., Schneider, R.L., Walter, M.T., 2016. Nutrient Cycling in Grassed Roadside Ditches and Lawns in a Suburban Watershed. *J. Environ. Qual.* 45, 1901.

O'Dell, J.W., 1993. Determination of nitrate-nitrite nitrogen by automated colorimetry. *Method 353.2*.

Pluer, W. T., Geohring, L.D., Steenhuis, T.S., Walter, M.T., 2016. Controls influencing the treatment of excess agricultural nitrate with denitrifying bioreactors. *J. Environ Qual.* 45, 772–778.

Robertson, W.D.D., Vogan, J.L.L., Lombardo, P.S.S., 2008. Nitrate Removal Rates in a 15-Year-Old Permeable Reactive Barrier Treating Septic System Nitrate. *Ground Water Monit. R.* 28, 65–72.

Schipper, L.A., Robertson, W.D., Gold, A.J., Jaynes, D.B., Cameron, S.C., 2010. Denitrifying bioreactors—An approach for reducing nitrate loads to receiving waters. *Ecol. Eng.* 36, 1532–1543.

Schneider, R. Marino, R. 2015. Coupling in-ditch studies and modeling to understand

the landscape – wide nitrogen transport and denitrification potential of roadside ditch networks across catchments. *New York State Water Resources Institute Report*.

Seitzinger, S., Harrison, J.A., Böhlke, J.K., Bouwman, A.F., Lowrance, R., Peterson, B., Tobias, C., Van Drecht, G., 2006. Denitrification across landscapes and waterscapes: a synthesis. *Ecol. Appl.* 16, 2064–2090.

Shields, C.A., Band, L.E., Law, N., Groffman, P.M., Kaushal, S.S., Savvas, K., Fisher, G.T., Belt, K.T., 2008. Streamflow distribution of non-point source nitrogen export from urban-rural catchments in the Chesapeake Bay watershed. *Water Resour. Res.* 44, 1–13.

Tanner, C.C., Sukias, J.P.S., Headley, T.R., Yates, C.R., Stott, R., 2012. Constructed wetlands and denitrifying bioreactors for on-site and decentralised wastewater treatment: Comparison of five alternative configurations. *Ecol. Eng.* 42, 112–123.

CHAPTER 6

CONCLUSIONS ON DENITRIFYING BIOREACTOR TREATMENT OF STORMWATER

These studies show high potential for nitrate (NO_3^-) removal in stormwater using denitrifying bioreactors. All studies, agricultural, lab-scale, submerged, and ditch bioreactors, showed exceptionally high removal rate (RR) during elevated flow rates, however, removal efficiency (RE) often decreased. This suggests that high RR was driven by high flow rate and not by increased rates of denitrification. While RR peaked during high flow, it also decreased following storms, suggesting some disturbance within bioreactors that was supported by statistical models of field data. Analysis of flows showed that this was most prevalent in bioreactors that demonstrated more preferential flow than distributed flow patterns. None of the identified storm hydrograph characteristics was a strong indicator of bioreactor performance. Further work is necessary to better understand bioreactors response to storms in order to predict RR and inform design recommendations. This includes monitoring dissolved organic carbon and microbial community flushing, internal flow patterns at larger scales, and effect volume. Better designs should decrease negative impacts of disruption so that bioreactors maintain high RR.

Both novel applications studied here showed higher RR than the agricultural bioreactors, the highest of which was the submerged bioreactors in the wet detention ponds. These effectively removed almost all of the NO_3^- and potentially benefited from the constant rate and facilitation of denitrification beyond the bioreactor boundaries. Due to design differences between traditional agricultural bioreactors and

the novel applications, estimates of RR may not be the most effective at describing bioreactor effectiveness. However, both showed reduced NO_3^- concentrations that suggest bioreactors are an effective management practice for NO_3^- removal. Bioreactors are easily adaptable and capable of retrofit into existing stormwater infrastructure. Potential additional applications include bioretention, infiltration basins, and swales.